Concept controlling model for arresting epidemics, including COVID-19

Kaminskiy G. D.[a,*], Prostov Yu. I.[a], Prostov M. Yu.[a], Pimenov N. N.[a], Veselova E. I.[a], Vinokurov A. S.[a], Karamov E. V.[a,b], Panova A. E.[a], Turgiev A. S.[a,b], Chernetsova V. V.[c], Lomovtsev A. E.[d], Vasilyeva I. A.[a]

[a] *Federal State Budgetary Institution "National Medical Research Center of Phthisiopulmonology and Infectious Diseases" of the Ministry of Health of the Russian Federation, 4, bld. 2 Dostoevskaya, Moscow, 127473, Russia*
[b] *Federal State Budgetary Institution "National Research Centre for Epidemiology and Microbiology named after the Honorary Academician N. F. Gamaleya" of the Ministry of Health of the Russian Federation, 18 Gamalei, Moscow, 123098, Russia*
[c] *National Research University "Moscow Power Engineering Institute", 17, bld.3 Krasnokazarmennaya, Moscow, 111250, Russia*
[d] *The Department of Federal Service for Surveillance on Consumer Rights Protection and Human Wellbeing for Tula Region, 114 Oboronnaya, Tula, 300045, Russia*

Abstract

This article focuses on the assessment of the intensity of the epidemic process and the proportionate intensity of control by using mathematical modeling. In this work we studied the specifics of the parameters of the infectious and epidemic process, as well as control parameters. Formulas for controlling the epidemic process for calculating the critical levels of influence (interventions) and the time to achieve the result are obtained. A concept controlling model has been developed for both new and returning infectious diseases. The adequacy of the model based on real data, as well as examples of intervention campaigns are presented.

Keywords: epidemic control, threshold, intervention, parameters of epidemic process, mathematical model

[*] gregkaminski.gk@gmail.com

1. Introduction

1.1. Principles of the mathematical theory of epidemics

The mathematical theory of the spread of infectious diseases is a rapidly advancing science (Anderson et al., 2004; Fraser et al., 2004). It enables the understanding of epidemic process development (Koivu-Jolma and Annila, 2018). The focus on the mathematical theory of the spread of infectious diseases has increased in relation to the COVID-19 pandemic (Biggerstaff et al., 2020; Ferretti et al., 2020; Shao and Wo, 2020).

Both the simplest and the most complex models have been proven effective.

The classical background is the model of Kermack and McKendrick (Kermack and McKendrick, 1927).

It was shown that the differential epidemic models (that suggest an exponential distribution of infectiousness profiles) are excellent at describing recurrent measles epidemics (Cauchemez and Ferguson, 2008). Agent-based models implemented on supercomputers demonstrated high efficacy for COVID-19 across territories and among various population groups (Datta et al., 2022; Zatsepin et al., 2021). These models of epidemics appeared to be quite similar to the physical models of the distribution of elementary particles.

Mathematical modeling of the epidemic process is used to monitor and to affect the infectious disease incidence (Zumla et al., 2017).

In the 1960s the World Health Organization (WHO) developed models and methods for combating infectious diseases that could cause a public health emergency of international concern. These infections are highly contagious and lethal, and can trigger pandemic. The International Health Regulations (IHR) were first adopted at the 22nd Session of the WHO on July 26, 1969. Most of these infections require governmental control in order to restrict the movement of potentially infected people (WHO, 2005).

Modern epidemiology operates in terms of emerging and re-emerging diseases. This approach takes into account the evolutionary potential of pathogenic microorganisms and the dynamic relationship between microorganisms, hosts and the environment (Morens et al., 2004).

A set of methods for epidemic control is given in the Control of Communicable Diseases Manual (Heymann, 2008), formerly Control of Communicable Diseases in Man (Benenson, 1981).

The control is aimed at ensuring new cases reduction until the complete disappearance in the area Beliakov (1974). The term "intervention" can be used as a synonym, sharpening an interventional approach to ensure the infectious safety (Matsuki and Tanaka, 2019).

The modeling of an epidemic process is applied both to describe the natural course of an epidemic and to inform effective interventions (Knock et al., 2021). The emergence of effective vaccines has led to the global (smallpox) and regional (poliomyelitis, measles, diphtheria) eradication of infectious diseases. A special theory of vaccination control was developed. Models are used to justify the need for vaccination for a particular infection (Brauer and Castillo-Chavez, 2019).

Appropriate vaccination results in disease eradication, limited vaccination - in sudden outbreaks (Anderson and May, 1992). Special works are dedicated to global disease eradication programs (Thompson and Kalkowska, 2020).

Mathematical models help to define the cost-efficacy of various ways to control the epidemic process, including vaccination of the population (Arifin et al., 2019) and the gaps of control (Cutts et al., 2020).

Of great significance are works on modeling the epizootic process (a spread of the infectious disease in animals) with detection of infectious-immunological regularities during recurrent epidemics (Atkins et al., 2013).

An important method of the control is the timely identification, isolation and treatment of sources of infectious agents, as well as contact tracing. Recently, works on mathematical modeling of this type of control were done (Sturniolo et al., 2021). The COVID-19 epidemic has shown the importance of non-pharmaceutical interventions with two distinct strategies: suppression and mitigation (Ferguson et al., 2020). Special works focus on lockdown modeling (Padmanabhan et al., 2021).

1.2. Types of epidemic models

Currently, there is no single model of epidemics and are only a few works on proving the comparability of some models with others. Besides, the areas of applicability of each of the models have not been sufficiently studied either: for example, which model is relevant for describing the dynamics in the equilibrium, and which model describes outbreaks or drops in incidence far from the stationary state; what the difference is in the shapes of epidemic curves in various models. In most cases, models have many parameters that are sometimes redundant. Types of epidemic models are explained in Table 1.

Table 1: Types of epidemic models.

Model	Use and features of the model	Use and features of the model
1	Differential Model	This model contains differential equations for the categories of susceptible, exposed (individuals in the latent phase), infected, quarantined, immune, treated, vaccinated, and deceased. This type also includes structured models that describe epidemics in each city (territory) using separate systems of differential equations and contain a matrix established of connections between cities (territories) (Aronna et al., 2021; Cano, 2020; Demongeot et al., 2020). Parameter profiles are exponential in time.
2	Integral Model	This is the most accurate model computationally, as the infectiousness profile is documented by days of illness. Special profiles are used to show the loss of immunity and timely case detection with subsequent neutralization. The number of new cases of diseases in the Integral Model is determined by the formula: $$A(t) = R\left(\int_0^T A(t-\tau)e^{-\mu\tau}\rho(\tau)d\tau\right)X(t)$$ $A(t)$, disease incidence; $\rho(\tau)$, infectiousness profile (standardized), $\int_0^T \rho(\tau)d\tau = 1$; μ, inflow/outflow of susceptible individuals; R, contact rate (secondary attack rate). The Integral Model is sometimes equivalent to the Multiclass Differential Model or the Model of Delay Differential Equations (Feßler, 2020; Fodor et al., 2020).
3	Territorial Agent-Based Model	The Agent-Based Model properly describes the slow changes of transmission activity and incidence. There is no contact rate (R) in the Territorial Agent-Based Model. Instead, there is the likelihood of encounters of infected and susceptible individuals and the likelihood of being infected during a single exposure. It is matched to the area, infrastructure, and social categories and age groups of the population. Both the Territorial Agent-Based Model and the Integral Model enable distributed profiles (by day). This Model is more precise in describing some types of dynamics, specifically sites of chain-binomial infection transmission (Silva et al., 2020).
4	Randomized Model	This is a variant in Models 1-4, where at each step the contact rate R, the inflow of susceptible μ, and the number of newly infected are shown as randomly distributed. This Model provides expected means as well as upper and lower confidence limits (Chen-Charpentier and Stanescu, 2010; Popkov et al., 2021).
5	Models based on the Mean Field Game Theory	This Model is based on a coupled pair of partial differential equations: the Fokker-Planck (Kolmogorov) Equation that evolves forward in time and determines the distribution of interacting subjects over the state space; and the Hamilton-Jacobi-Bellman Equation that evolves back in time and defines if the chosen strategy is optimal (Bensoussan et al., 2013; Gao et al., 2021).

2. The aim and objectives of the study

The aim of this work is to create concept controlling model of the epidemic process to assess the intensity of the epidemic process (force of infection), determine the severity of transmissibility and the proportionate neces-

sity/intensity of control.

This model should describe at least two-term parasitic systems that consist of two interacting populations, a parasite and a host (models with transmitters and preservation in the environment are more complex by definition).

The model should qualitatively and quantitatively describe the epidemic process of the main infections. As some dangerous infections (eg. HIV-infection) have intensive disease caused death rate, the model should operate in varying population size. So variables should be given in absolute numbers.

The equations in the model should provide obtaining control formulas that are convenient in practical use.

Arresting epidemics should be achieved through various control components. Combined effects for control are valued.

3. Construction of the model

3.1. Selection and specification of the parameters of the infection and epidemic process

The contact rate (the basic reproductive rate) R is the main parameter of an epidemic process (Guerra et al., 2017). It shows how many susceptible people become infected from one infected person, subject to the general susceptibility of the population. The larger R, the greater the rate of development and the level of the disease incidence of the population. Despite the strong selective pressure that favors the reproduction of more virulent parasites, the R parameter does not indefinitely increase. The concept of trade off was developed (Alizon and van Baalen, 2005; Alizon et al., 2009) in order to explain this pattern, but the reasons for this phenomenon have not been fully studied.

The contact rate is a multi-faceted parameter that reflects biological (pathogen virulence), environmental (population crowding, waste water levels) and social factors (security and restrictive measures, including a lockdown).

There are estimates of the contact rate R depending on the nosology (Anderson, 1982, 2013). The work also showed a significant variability of R within infections (nosologies). Therefore, the contact rate R should be recognized as variable depending on the territories, population groups, and timeframe. The contact rate R can be estimated both in epidemic fo ci (Shah et al., 2020) and by solving the inverse problem of reproducing the dynamics using incidence curves (Hadeler, 2011).

The intensity of infection (infectiousness) parameter α defines the duration of an infection process (Zhou et al., 2019). The associated parameter is the intensity of recovery β. In infections without death rate $\alpha = \beta$. If the death rate ϵ exists $\alpha = \beta + \epsilon$. If there is no cure, the man is dangerous as the cause of infection for the whole life $\alpha = \mu, \beta = 0$.

The population natural outflow is denoted by the parameter μ. When considering an organized population with the internal (in the risk group) circulation of a pathogen, the parameter μ has the meaning of the inverse time spent in the group (for example, the time spent in a preschool institution, the time spent at school). In this case, an adjustment is needed because, for example, some children come to school with immunity developed in the kindergarten. Also, for some infections, the parameter μ has the meaning of being at risk; for example, it is known that the average time spent in a population of intravenous psychoactive substance users is 2-5 years, that includes narcotic dependent high death rate.

In childhood infections, the parameter μ is determined by the average age of the patients.

Groups with high and partial renewal (for example, military groups) are of particular epidemiological danger; in these groups, the highest levels of disease incidence are formed.

The population outflow parameter is the relative coefficient as it is multiplied on the variable value.

The population inflow parameter is an absolute value and denotes the number of humans entering the population each day. In childhood infections it is the number of the everyday births. For convenience it is designated as $N\mu$, were N is the real integer.

The coefficient of loss of immunity k is another essential parameter. In infections with lifelong immunity, it equals zero (measles). The mean value of this ratio for COVID-19 is 0.0055 (1/180 days) Cevik et al. (2021). The high value of the coefficient of loss of immunity determines the greater value of disease incidence.

3.2. Selection and specifics of control parameters

In systems of physics and technology, there is a clear understanding of control, with effective control always implying the achievement of a target value by selecting the right trajectory. In epidemiological systems this is a challenge. In global terms, the control of an epidemic process is a system of targeted impacts that result in a systematic decrease in the infection

incidence of the population, up to interruption of epidemic process and elimination of disease.

The main control parameter is the intensity of vaccination (and pre-exposure prophylaxis) of those susceptible λ_1 and recovered λ_2. The λ_2 parameter is used for infections with loss of immunity.

Control through isolation, detection and treatment is divided into two parts: δ_1 - for those with acute infection, δ_2 - for those who are carriers. Finding and treating carriers is of great value, because without this arresting epidemics is impossible.

The impact on the transmission mechanism is revealed by control coefficient r, that makes the effective contact rare to be rR. These measures include all ways to diminish effective contacts, i.e. lockdown, inter-group isolation, secure behaviour, sanitary measures.

Note 1. *Infected people are identified using clinical, epidemiological and laboratory methods. Clinical methods involve the identification of intense symptoms of a disease (fever, intoxication, anosmia and ageusia). Epidemiological methods involve reducing the search to individuals in direct contact or potential contact (a risk group). Laboratory methods include testing for DNA/RNA and/or antigen of the infectious agent. In order to more extensively identify the sources of infectious agents, including early in the disease, the environment of sources of infectious agents is tested, and there is repeated testing (screening, saturation), including the use of non-invasive tests.*

Note 2. *Treatment of identified cases leads to a decreased concentration of the pathogen in the person's body and a decreased infecting activity and decreased spread of the disease. For some infections, it is possible to isolate the identified patient at home or in the hospital. In this case the person moves to the class Q - quarantined.*

Note 3. *Prevention of infection in susceptible individuals includes vaccination and prophylactic treatment (pre- and post-exposure). Vaccination involves revaccination that immunity is retained.*

Note 4. *The impact on the transmission mechanism includes measures in relation to the human environment (eg. restoring safe water supply), as well as security and restrictive measures (for example, the introduction of a lockdown). Susceptible individuals are kept out of the infected area.*

3.3. Model variables and differential equations

The system of equations of the epidemic process under conditions of sufficient control resources – **concept controlling model** - comprises 7 independent differential equations, depicting dynamics of major 7 variables:

$$\begin{cases} S(t)' = -\dfrac{rS(t)(R_1\alpha_1 A(t) + R_2\alpha 2C(t))}{S(t)+E(t)+A(t)+C(t)+R(t)+V(t)} + \\ + \mu N - \mu S(t) + k_1 R(t) + k_2 V(t) - \lambda_1 S(t) \\ E(t)' = \dfrac{rS(t)(R_1\alpha_1 A(t) + R_2\alpha_2 C(t))}{S(t)+E(t)+A(t)+C(t)+R(t)+V(t)} - (\gamma_1+\mu)E(t) \\ A(t)' = \gamma_1 E(t) - (\beta_1+\gamma_2+\epsilon_1+\delta 1+\mu)A(t) \\ C(t)' = \gamma_2 A(t) - (\beta_2+\epsilon_2+\delta_2+\mu)C(t) \\ R(t)' = \beta_1 A(t) + \beta_2 C(t) + \delta_3 Q(t) - (\lambda_2 + k1 + \mu)R(t) \\ V(t)' = \lambda_1 S(t) + \lambda_2 R(t) - (k2+\mu)V(t) \\ Q(t)' = \delta_1 A(t) + \delta_2 C(t) - (\delta_3+\mu)Q(t) \end{cases} \quad (1)$$

See the compartmental diagram associated to this model in Fig. 1.The 8th variable is dependent from the others and include humans that left the population and died because of the infection and natural sauces (class DW - dead and withdrawn). Before treatment the ill persons are identified and isolated, forming class Q. So these persons, as well as DW class persons, are not presented for the interaction as contacts, no potentially effective (S), no potentially ineffective (classes *E, A, C, R, V*). It is very important not to put classes DW and Q in mass action. As the model is in the absolute numbers, the absolute number of susceptible numerator *S(t)* should have the denominator *S(t)+E(t)+A(t)+C(t)+R(t)+V(t)* to show the probability of contacts of infected and susceptible. Thus the model has well posed mass action in case the general population size is changing, either growing up, or being stable, or moving down.

The variables, the parameters of the infection and epidemic process, and control parameters are given in Table 2.

Table 2: Variable and parameters of the concept controlling model.

Designation	Description
Variables	
S	susceptible
E	exposed, but not yet infectious
A	acute infected
C	chronically infected (carriers)
R	immune - resistant
V	immune - vaccinated
Q	isolated for treatment - quarantined
Parameters	
α_1	the intensity of infection of acute infected
α_2	the intensity of infection of chronically infected
β_1	the intensity of recovery of acute infected
β_1	the intensity of recovery of chronically infected
γ_1	the intensity of transition to acute infection
γ_1	the intensity of transition to chronic infection
k_1	the intensity of natural immunity loss
k_2	the intensity of vaccine immunity loss
ϵ_1	the death rate of acute infected
ϵ_1	the death rate of chronically infected
R_1	the contact rate of acute infected
R_2	the contact rate of chronically infected
μ	the intensity of outflow
μN	the intensity of inflow
Control coefficients (control intensity coefficients)	
λ_1	intensity of vaccination of susceptible and pre-exposure prophylaxis
λ_2	the intensity of vaccination of recovered
δ_1	intensity of detection, isolation and treatment of acute infected
δ_2	the intensity of detection, isolation and treatment of chronically infected
δ_3	the intensity of return from isolation with immunity
r	the the added control component for the contact rate through the implementation of security and sanitation measures

Variables: S is the number of susceptible, E is the number of exposed but not yet infectious, A is the number of acute infected, C is the number of chronically infected, R is the number of resistant, V is the number of having vaccine immunity, Q is the number of isolated for treatment (quarantined).

Parameters of the infection process: α is the intensity of infection, β is the intensity of recovery, k is the intensity of immunity loss, ϵ is the death rate, associated with the infectious disease.

Parameters of the epidemic process: R is the contact rate, μ is the intensity of outflow, μN is the intensity of inflow.

Control coefficients (control intensity coefficients): λ_1 is the intensity of vaccination of susceptible and pre-exposure prophylaxis, λ_2 is the intensity of vaccination of recovered (they may have potentially lost their immunity and therefore need to be vaccinated), δ_1 is the intensity of detection, isolation and treatment of acute infected, δ_2 is the intensity of detection, isolation and treatment of chronically infected, r is the the impact on the contact rate with an added control component through the implementation of security and sanitation measures.

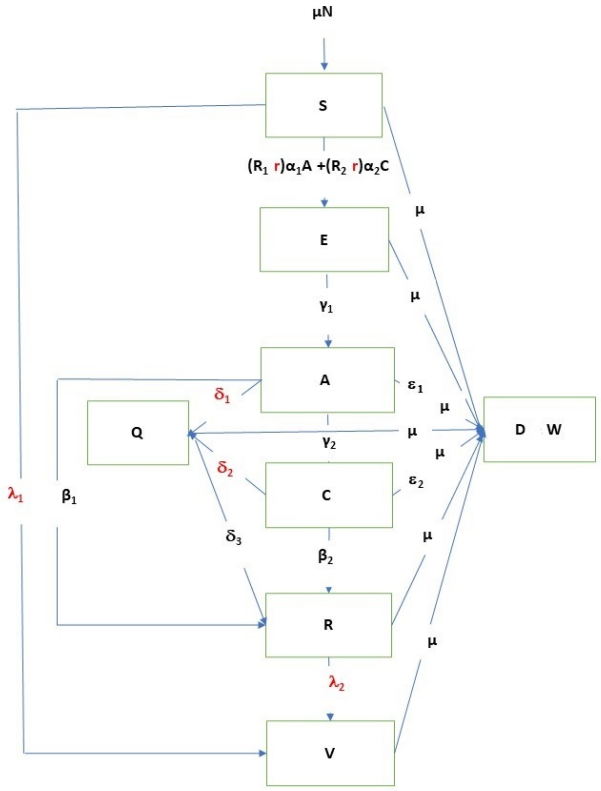

Figure 1: Model diagram.Variables are in blocks, epidemic and infection parameters are in black, control parameters are in red.

In order to obtain seasonal variation, seasonal prevalence should be added for contagiousness of acutely and chronically infected:

$$\begin{cases} R_1 = R_1 0 \left(1 + \iota \sin\left(\dfrac{2\pi t + \theta}{T}\right)\right) \\ R_2 = R_2 0 \left(1 + \iota \sin\left(\dfrac{2\pi t + \theta}{T}\right)\right) \end{cases} \tag{2}$$

Parameters of the epidemic process: ι – the intensity of seasonal oscillations, θ – the duration of the phase shift indicating the seasonal maximum, T – the dimension (observation interval: 365.25 days, 12 months, 52.18 weeks). The above system depicts the number of new cases, got from acutes and carriers.

The absolute number of new cases is

$$\frac{rS(t)(R_1\alpha_1 A(t) + R_2\alpha 2C(t)}{S(t) + E(t) + A(t) + C(t) + R(t) + V(t)}$$

The main control parameter is the vaccination of susceptible $S(t)$ with intensity λ_1. Clearly both vaccination and re-vaccination are needed for lifelong immunity to form. The model for $k \neq 0$ also suggests vaccination for recovered patients. The intensity of vaccination of recovered patients is denoted as λ_2. In some cases, people are vaccinated without clinically and serological data on past disease. In this case, $\lambda_1 = \lambda_2$.

When the period of isolation is over, treated persons assumed to return with immunity.

The system of the epidemic process operates in absolute numbers.

3.4. Properties of the system

The trivial stationary solution of the differential equation system (1):

$$E1 = A1 = C1 = Q1 = 0$$
$$S1 = \frac{(k_2 + \mu)N}{k_2 + \lambda_1 + \mu}$$
$$V1 = \frac{N\lambda_1}{k_2 + \lambda_1 + \mu}$$

The Jacobian matrix for the trivial solution Jac 1 is shown on figure 2.

$$Jac1 = \begin{bmatrix} -\mu - \lambda 1 & 0 & -\frac{r\,(k2+\mu)\,N\,\alpha 1\,l}{(k2+\lambda 1+\mu)\left(\frac{(k2+\mu)\,N}{k2+\lambda 1+\mu}+\frac{N\,\lambda 1}{k2+\lambda 1+\mu}\right)} & -\frac{r\,(k2+\mu)\,N\,\alpha 2\,m}{(k2+\lambda 1+\mu)\left(\frac{(k2+\mu)\,N}{k2+\lambda 1+\mu}+\frac{N\,\lambda 1}{k2+\lambda 1+\mu}\right)} & k1 & k2 & 0 \\ 0 & -\gamma 1 - \mu & \frac{r\,(k2+\mu)\,N\,\alpha 1\,l}{(k2+\lambda 1+\mu)\left(\frac{(k2+\mu)\,N}{k2+\lambda 1+\mu}+\frac{N\,\lambda 1}{k2+\lambda 1+\mu}\right)} & \frac{r\,(k2+\mu)\,N\,\alpha 2\,m}{(k2+\lambda 1+\mu)\left(\frac{(k2+\mu)\,N}{k2+\lambda 1+\mu}+\frac{N\,\lambda 1}{k2+\lambda 1+\mu}\right)} & 0 & 0 & 0 \\ 0 & \gamma 1 & -\beta 1 - \gamma 2 - \epsilon 1 - \delta 1 - \mu & 0 & 0 & 0 & 0 \\ 0 & 0 & \gamma 2 & -\beta 2 - \epsilon 2 - \delta 2 - \mu & 0 & 0 & 0 \\ 0 & 0 & \beta 1 & \beta 2 & -k1 - \mu - \lambda 2 & 0 & \delta 3 \\ \lambda 1 & 0 & 0 & 0 & \lambda 2 & -k2 - \mu & 0 \\ 0 & 0 & \delta 1 & \delta 2 & 0 & 0 & -\delta 3 - \mu \end{bmatrix}$$

Figure 2: Jacobi matrix for trivial stationary solution

The characteristic polynomial is multistory, however all 7 coefficients were obtained, simplified and compared.

Formula 1.

$$r > \frac{(\lambda_1 + k_2 + \mu)(\gamma_2 + \epsilon_1 + \mu + \beta_1 + \delta_1)(\gamma_1 + \mu)(\beta_2 + \epsilon_2 + \delta_2 + \mu)}{(R_1(\beta_2 + \epsilon_2 + \delta_2 + \mu)\alpha_1 + R_2\alpha_2\gamma_2)\gamma_1(k_2 + \mu)}$$

In this very case all 7 coefficients of characteristic polynomial of Jac 1 are positive and the trivial stationary condition is stable (the infection is cured out), otherwise at least one coefficient is negative, that means that the trivial condition is unstable and the infection persists.The result does not depend on component N of inflow μN, coefficient of immunity loss k_1, isolation release intensity δ_3. However time to result to zero cases may depend on these parameters.

If the control conditions are near the threshold, it takes much time to clear out the infection. If the control conditions are above, but near the treshold, it takes much time to clear out the infection. This happens especially in case of chronic infections, infections with carriers and with temporary immunity, that interferes with reaching the trivial equilibrium. Concrete time and target concentration of infected can be obtained by simulations. However the formula for controlling the epidemic process was obtained. It comprises levels of impact (intervention) at which the epidemic process ends - condition for arresting the epidemic process, as well as time to result and target concentrations.

In this formula t is the time of reaching the critical concentration n of the source of infection, δ is the intensity of revealing and treatment of cases, λ - the intensity of vaccination.The formula allows to find pairs δ and λ to arrest epidemic process in the scope of the certain period of time. The derivation of the formula is given in appendix B.

Formula 2.

$$\delta = ((RI_0\alpha - k)((k+\lambda+\mu)^2(RY_0\alpha+\lambda+\mu)^2 ln(I_0/n) - R^2 I_0((Y0-1)(\mu t+1)k^2+$$
$$+((2t\mu^2+(\beta t+2\lambda t+1)\mu+\lambda t\beta+\lambda+\beta)I_0-(2(\lambda+\mu)(t\mu+(1/2)S_0+1/2))k+$$
$$+(\lambda+\mu)^2(t(\mu+\beta)I_0-t\mu-S_0))\alpha^2-2(((t\mu^2+(\lambda t+(1/2)t\beta+1/2)\mu+$$
$$+(1/2)\lambda t\beta+(1/2)\lambda+(1/2)\beta)I_0-(1/2)\lambda-(1/2)\lambda t\mu-(1/2)t\mu^2)k^2+$$
$$+2(\lambda+\mu)((t\mu^2+(\lambda t+(3/4)t\beta+1/4)\mu+3\lambda t\beta(1/4)+$$
$$+(1/4)\lambda+(1/2)\beta)I_0-(1/2)t\mu^2+(-(1/2)\lambda t-(1/4)S_0+1/4)\mu-(1/4)(S_0+1)\lambda)k+$$
$$+(\lambda+\mu)^2(t(\mu+\beta)(\lambda+\mu)I_0-(1/2)t\mu^2+$$
$$+(-(1/2)\lambda t-(1/2)S_0+1/2)\mu-(1/2)S_0\lambda))R\alpha-t(\lambda+\mu)^2$$
$$(k+\lambda+\mu)^2(\mu+\beta))e^{t(RI_0\alpha+k+\lambda+\mu)}-(-k(RI_0\alpha+\lambda+\mu)^2$$
$$((S_0+I_0-1)k+(\lambda+\mu+\beta)I_0+(S_0-1)(\lambda+\mu))$$
$$e^{RI_0\alpha t}+(k+\lambda+\mu)^2(R^2S_0I_0^2\alpha^2+I_0((I_0-1)k+(S_0-1)\mu+S_0\lambda)R\alpha+$$
$$((\lambda+\mu+\beta)I_0-\lambda)k)e^{tk})R\alpha)/$$
$$/((((\lambda t+\mu t+1)k+t(\lambda+\mu)^2)R^2I_0^2\alpha^2+(2(\lambda+(1/2)k+\mu)$$
$$((\lambda t+\mu t+1)k+t(\lambda+\mu)^2)RI_0\alpha+t(\lambda+\mu)^2(k+\lambda+\mu)^2)$$
$$(RI_0\alpha-k)e^{(t(RI_0\alpha+k+\lambda+\mu)}-$$
$$-((RI_0\alpha+\lambda+\mu)^2e^{RI_0\alpha t}-e^{tk}(k+\lambda+\mu)^2)Rk\alpha I_0)$$

Rule 1. *The greater the influence of vaccination and pre-exposure prophylaxis and the more intensive the identification and restriction of sources of the infectious agent, the less amount of lockdown is needed. The higher the level of vaccination and pre-exposure prophylaxis, the lower can be be the level of detection of sources of the infectious agent.*

The counterbalances: between control parameters, between control parameters ans time to result - are depicted in epidemic graphs as the auxiliary tool to visualize the necessary forces to arrest the epidemic.

3.5. Epidemic diagram (colored epidemic graph)

Epidemic diagram visualizes the epidemic control formula and shows conditions of loosing the stability between major control parameters: r, δ (δ_1 and/or δ_2), λ (λ_1 and/or λ_2).

The epidemic diagram (epi-diagram) clearly represents a function of two arguments, namely, the values of exposure to the contact rate r, depending on the intensity of detection, isolation and treatment of sources of infection δ and the volume of vaccination λ. An example diagram is shown in Fig. 3. With a high intensity of δ and λ decreasing the contact rate of infection (for example, lockdown) is not required (r=0, blue color). At low intensity of δ and λ, a vivid decreasing of contact rate of infection is demanded ($r = 1.6$, yellow color).

Thus, the colored epidemic graph shows that with significant efforts to identify the sources of infection and vaccination, the levels of lockdown may be lower. The diagram is digital and shows concrete values.

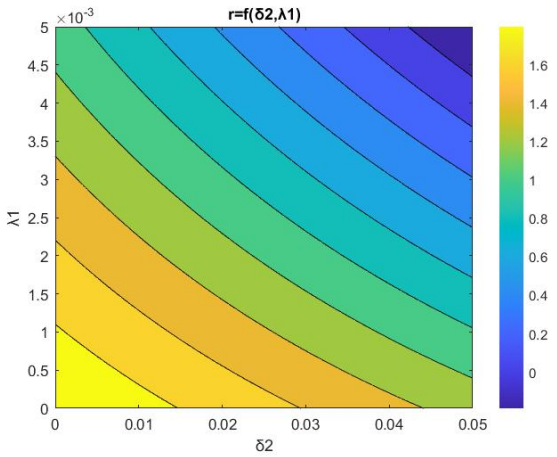

Figure 3: Epidemic diagram (colored epidemic graph). For infections with parameters $R = 3$, $\mu = 0.000157$, $\alpha = \beta = 0.074$, $k = 0.0055$, $\lambda_2 = 0.0001$, δ_1=0.

3.6. Epidemic corridor

To form the epidemic corridor from time to target equation, two boundary control conditions are laid down: 1 – with the maximum severity of the control parameters r, δ, λ; 2 – with the minimum but relevant severity of the control parameters r, δ, λ. The intersection of these curves with the abscissa axis represents the time to reach the target (the minimum concentration of sources of the causative agent of infection) under the condition of minimum and maximum control intensities. In the Fig. 4, the minimum achievement time was 200 days, the maximum achievement time was 500 days. During the implementation of the intervention program, the intensity of the control

parameters varies, but the control trajectory remains within the epidemic corridor. When compensating for the insufficient impact of one of the parameters on other parameters, the control trajectory is located in the middle of the epidemic corridor.

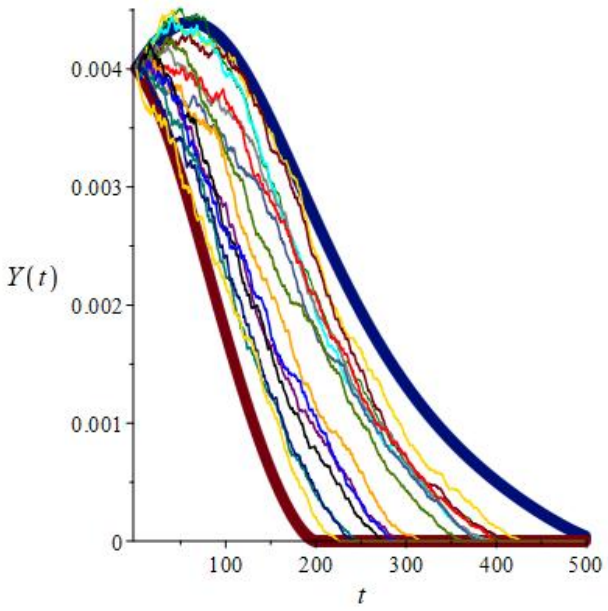

Figure 4: Epidemic corridor. For infections with parameters $R = 5.1$, $\mu = 0.000273973$, $\alpha = \beta = 0.071428571$, $k = 0.0001$, $\lambda_{min} = 0.0001$, $\delta_{min} = 0.0001$, λ_{max}=0.0002, $\delta_{max} = 0.0002$.

Thus, epidemic graphs demonstrate interchangeability of the control parameters and enhancement to reach the target in a better time.

3.7. Epidemic cube

Epidemic cube is the another form of epidemic diagram. The element of the cube is the time to result. The target result is the condition with less than 1 infected person for the the period of maximum infection length. Corresponding epidemiological diagram is shown on Fig. 5.

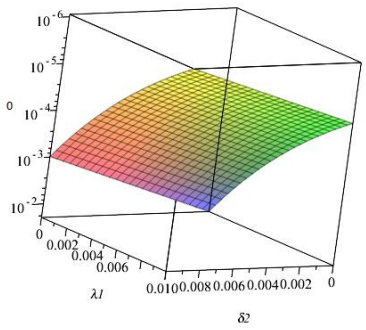

Figure 5: The epidemiological diagram: interdependencies between detection and restriction of pathogen sources δ_2, vaccination λ_1, order diminishing infected population o. Time to target concentration $t = 300$ days. $\mu = 0.00157$; $R = 3$; $k = 0.0055$; $\mu = 0.00157$; $\lambda_2 = 0.0001$; $\alpha = \beta = 0.074$, $\delta_1 = 0$, $Y_0 = 0.005$, $X_0 = 0.33$.

Defining target number (concentrations) of infected people that is less than the individual means the local elimination.

Thus, control is active and aggressive. It should cover all possible control parameters, with a predetermined intensity based on calculations, to achieve the goals of stopping the epidemic process. If all three control factors remain at a higher level, the time to interrupt the epidemic process is reduced and arrest succeeds.

4. Use of the model to measure the epidemic force

4.1. Epidemic data and parameter estimation

The materials used were data received from medical organizations on the number of registered cases of eleven acute infections: measles, rubella, mumps, viral hepatitis A, influenza A, COVID-19, whooping cough, chicken pox, scarlet fever, Sonne dysentery, and gonorrhea; and two chronic infections (viral hepatitis C, HIV infection); a total of 13 infections. The observation period covered: measles – 60 years (1961-2021), rubella – 46 years (1975-2021), mumps – 60 years (1961-2021), viral hepatitis A – 51 years (1970-2021), influenza A – 29 years (1992-2021), COVID-19 – 665 days (03/01/2020-12/25/2021), whooping cough – 30 years (1991-2021), chicken pox – 30 years (1991-2021), scarlet fever – 33 years (1961-1994), Sonne dysentery – 30 years (1991-2021), gonorrhea – 30 years (1991-2021), viral hepatitis C – 30 years (1991-2021), and HIV infection – 30 years (1991-2021).

A total of 413,887 cases were analyzed: measles – 17,485, rubella – 18,049, mumps – 19,350, viral hepatitis A – 4,826, influenza A – 196,890, COVID-19 – 85,997, whooping cough – 1,558, chicken pox – 26,633, scarlet fever – 15,838, Sonne dysentery – 3,332, gonorrhea – 8,694, viral hepatitis C – 1,468, HIV infection – 13,767.

Data on measles, rubella, mumps, viral hepatitis A, chicken pox, and scarlet fever was collected in Novomoskovsk, Tula Region; data on influenza A, whooping cough, Sonne dysentery, and gonorrhea was collected in Tula; on viral hepatitis C and HIV infection in the Tula Region; on COVID-19 in Khasavyurt, Dagestan Region.

The observation interval for infections varied. Daily data was collected on influenza A and COVID-19; for measles, rubella, mumps, viral hepatitis A, whooping cough, chicken pox, scarlet fever, Sonne dysentery and gonorrhea the data was collected weekly; and on a monthly basis for viral hepatitis C and HIV infection.

The parameters of the epidemic process, namely the contact rate R, and the intensity of seasonal oscillations ι that indicates a seasonal maximum, were explored in the model for better comparison of the model data with real data. The duration of the phase shift θ was determined in accordance with average seasonal zenith incidence of a disease. The intensity of the group turnover μ was based on the borderline of the patient age and the belonging of disease to schools and pre-schools. Information about the parameters of the infection process α and k was taken from evidence-based literature and is presented in Appendix A.

The model data was compared to with real life data by calculating the Euclidean distance Q using the formula:

$$Q = \sqrt{\frac{\Sigma_0^P (I_t - M_t)^2}{P}}$$

where I_t is the actual value of the number of new cases for the observation interval t, M_t is the model value of the number of new cases for the observation interval t, P is the observation time.

The parameters were selected (optimized) by minimizing the Euclidean distance using the universal gradient descent method. The parameters were selected individually, pairwise and by group within the specified limits using 3-5 iterations Fazakas-Anca et al. (2021).

4.2. Aerosol infections with lifelong immunity

The weekly dynamics of the number of new cases of diseases (historical data) of measles, mumps, and chicken pox in a city with a population of 140 thousand people in the pre-vaccination period was analyzed (Novomoskovsk). Whooping cough was examined in a city with a population of 500 thousand people (Tula). The dynamics of the epidemic process of measles was monitored from 1961 to 1968 (7 years)/mumps from 1961 to 1984 (23 years)/chicken pox from 1991 to 2021 (30 years) and whooping cough from 1991 to 1995 (4 years). In this time frame, people were not vaccinated against these infections and the epidemic process developed as an autonomous system.

The diseases were mostly found in nurseries and primary school students. Accordingly, the average life expectancy in the group was 506.3 weeks, or 9.7 years ($\mu = 0.002$).

The number of nursery school children and primary school students who were in contact and involved in the airborne transmission of measles, mumps and chicken pox in Novomoskovsk (N) amounted to 18,000 people. The population involved in active contact with whooping cough in Tula was 3,000, as this infection often manifests as benign and subclinical Cherry (2013), and most cases of the disease occur in children under 5 years of age Greenberg et al. (2005).

The average life expectancy of a group of nursery school children was 313.2 weeks, or 6 years. The duration of infection (and, accordingly, recovery) with measles was 1.6 weeks (11 days), 3.1 weeks (22 days) with mumps, 3.0 weeks (21 days) with chicken pox and with whooping cough 2.7 weeks (19 days). These infections cause lifelong immunity ($k = 0$). The severity of seasonal oscillations ranged from 0.13 for measles to 0.45 for chicken pox. The maximum incidence of measles, mumps, and chicken pox was in January, and for whooping cough in September. The highest contagiousness was observed in measles ($R = 5.1$), the lowest in whooping cough ($R = 3.0$).

The parameters of the infection and epidemic process and the initial conditions for its development are given in Table 8.

Table 3: Parameters and initial conditions of the epidemic process of aerosol infections with lifelong immunity.

	Measles	Mumps	Chicken pox	Whooping cough
R	5.1	3.6	3.3	3.0
ι	0.13	0.24	0.45	0.20
θ	-40	-37	-37	-22
μ	0.002	0.002	0.002	0.003
k	0	0	0	0
α	0.636	0.318	0.33	0.368
β	0.636	0.318	0.33	0.368
N	18,000	18,000	18,000	3,000
S_0	3,600	5,400	4,500	990
A_0	45	20	90	8
T	52.18	52.18	52.18	52.18
Dimension	Week	Week	Week	Week

Fig. 6 shows the weekly dynamics of new cases of pediatric infection.

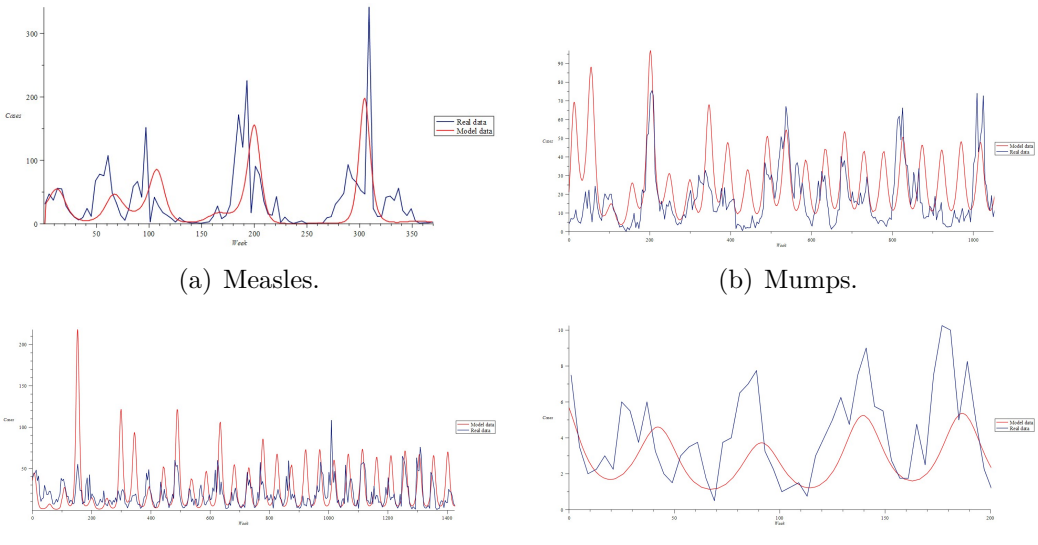

(a) Measles.

(b) Mumps.

(c) Chicken pox.

(d) Whooping cough.

Figure 6: Real data and model data of new cases of aerosol infections with lifelong immunity.

It can be seen in Fig. 6 that the model reproduces seasonal and cyclic os-

cillations in incidence, the latter being due to the superposition of sinusoidal disturbances on the frequency of the system. Measles has biennial peaks, as described in classic epidemiology papers Marguta and Parisi (2016).

The mumps incidence model reproduced a 3-4-year frequency, and the chicken pox model reproduced a 4-year frequency; however, the model curves are closer to stationary values by the end of the observation, while periodic oscillations continue according to the real data. The real systems of the epidemic process experience more perturbations.

Since the observation interval for whooping cough took 4 years, it is insufficient to assess the frequency, only seasonal prevalence can be clearly observed.

4.3. Aerosol infections with loss of immunity

The dynamics of rubella and respiratory streptococcal infection, scarlet fever, was studied in Novomoskovsk; influenza A in Tula; and COVID-19 in Khasavyurt, Dagestan Region, with a population of 146,000 people. The study of viral infections was complemented by the study of bacterial infection (*Streptococcus pyogenes*). The observation period covered 31 years (1975 to 2006) for the epidemic process of rubella, 24 years (1961 to 1985) for scarlet fever, 5 years (1992 to 1997) for influenza A, and 1.8 years (March 2020 to December 2021) for COVID-19.

The median group survival time for rubella and scarlet fever was 9.7 years, identical to other pediatric infections; it was 19-20 years for influenza and COVID in keeping with the age structure of the population at the time of observation. The population involved in active contact with rubella and scarlet fever was 18,000. Due to the larger population of the city, 60,000 people were involved in the active transmission of influenza, and 13,500 people were involved in COVID-191. The patient is contagious for 19 days with rubella, for 7 days with scarlet fever, 5 days with influenza, and 14 days with COVID-19. These infections may cause loss of immunity ($k \neq 0$). With rubella, relapses are possible but rare ($k = 0.000251$; 1/week). In the concept controlling model, the parameter k describes both loss of immunity and new antigenic variants of microorganisms. In scarlet fever ($k = 0.000383$; 1/week), in influenza A ($k = 0.00005$; 1/day). COVID-19 has a significant rate of loss of immunity ($k = 0.0055$; 1/day).

In rubella, seasonal oscillations are pronounced, with a peak in January. The maximum contagiousness of scarlet fever was observed in October, and

in September with influenza and COVID-19. The contact rate R ranged from 1.6 for scarlet fever to 5.7 for COVID-19.

Table 4: Parameters and initial conditions of the epidemic process of aerosol infections with loss of immunity.

	Rubella	Scarlet fever	Influenza A	COVID-19
R	2.4	1.6	4.4	5.7
ι	0.33	0.10	0.12	0.12
θ	-40	-26	200	200
μ	0.002	0.002	0.000137	0.000137
k	0.000251	0.000383	0.00005	0.0055
α	0.368	1	0.2	0.074
β	0.368	1	0.2	0.074
N	18,000	18,000	60,000	2,500
S_0	6,300	11,880	19,800	2,225
A_0	80	90	450	8
T	52.18	52.18	365.25	365.25
Dimension	Week	Week	Day	Day

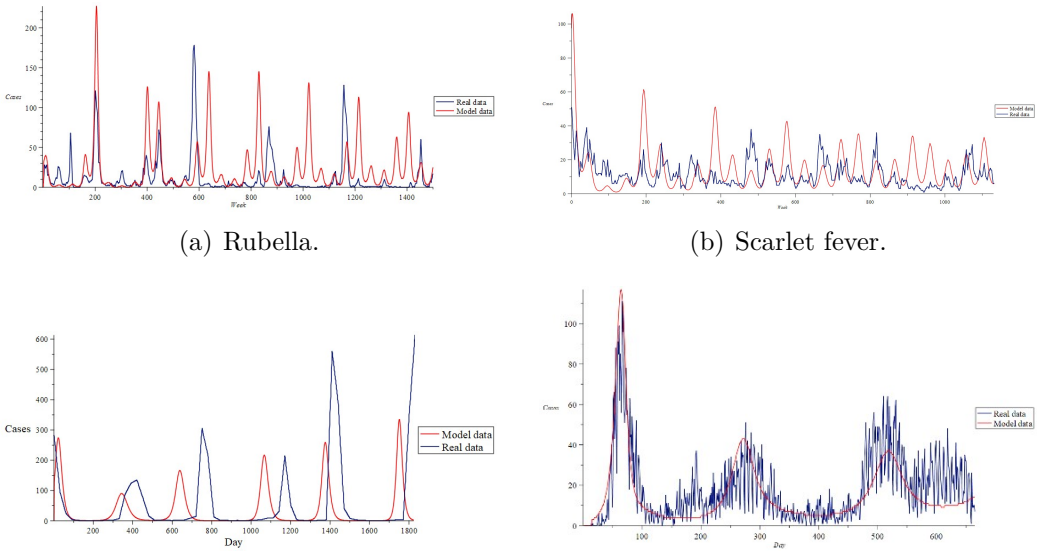

(a) Rubella.

(b) Scarlet fever.

(c) Influenza A.

(d) COVID-19.

Figure 7: Real and model data of new cases of aerosol infections with possible loss of immunity.

Now we shall consider in more detail the correspondence of the concept controlling model to the real data using rubella as an example. Rubella is an aerosol viral infection that mainly affects children aged 1 to 9 years. The medical and social significance of this infection is the impact on the fetus causing the development of encephalitis, insulin-dependent diabetes mellitus, and fetal death. The maximum data on observation in the pre-vaccination period (31 years) was obtained for this infection, so we shall reflect on it. Raises in incidence before the start of intervention campaigns (2007) were annually observed. For 31 years, there were 7 rises in incidence with the cycle duration 4 years.

The incidence before the start of the vaccination campaign remained dynamically stable and remained at a higher level. The model reproduces the dynamic stability (recurring epidemics) of rubella.

Yet, the superposition of peaks is not absolute: 4 rises coincide in time, and 3 rises do not coincide. However, there was a coincidence in the incidence rates. The cycle began in the area of high susceptibility of the population with a gradual increase in the incidence (over 2 years). A high rise begins with a significant off-season incidence in a susceptible population. After the high rise, there were two annual rises in the area of insusceptibility.

A partial phase mismatch is also noted in two other models, in respiratory streptococcal infection, scarlet fever and influenza; the variability of the pathogen is important with these infections, thus affecting model fitness.

Our research showed that in all infections except COVID-19 the starting point was near equilibrium. In COVID-19 the starting point was far from the equilibrium, the epidemic began in the presence of population sensitivity. A very good comparability of the real and model data was attained.

4.4. Enteric infections

The dynamics of the incidence of hepatitis A is presented for Novomoskovsk, and Sonne dysentery for Tula. The observation time for the dynamics of the incidence of hepatitis A was 27 years (1970 to 1997), and 8 years (1991 to 1999) for Sonne dysentery. These nosologies develop person to person transmission and often occur in organized groups of children. During the observation time, the maximum incidence was recorded in nursery school children and primary school students. The average lifetime of a group was 9.7 years.

The number of people involved in active contact with hepatitis A was 3,000 in Novomoskovsk, and 500 with Sonne dysentery in Tula, associated

with a more favorable epidemiological situation . The maximum contagiousness of hepatitis A and Sonne dysentery was observed in organized groups of children formed in early September (the "mixing" factor). The infectious period for hepatitis A was 28 days, and 10 days for Sonne dysentery. After hepatitis A, a stable immunity is formed; after dysentery, immunity lasts an average of a year. The contact rate for hepatitis A and Sonne dysentery was 2.9.

Table 5: Parameters and initial conditions of the epidemic process of enteric infections.

	Viral hepatitis A	Sonne dysentery
R	2.9	2.9
ι	0.40	0.20
θ	-19	-17
μ	0.002	0.002
k	0	0.02
α	0.25	0.70
β	0.25	0.70
N	3,000	500
S_0	1,020	250
A_0	70	20
T	52.18	52.18
Dimension	Week	Week

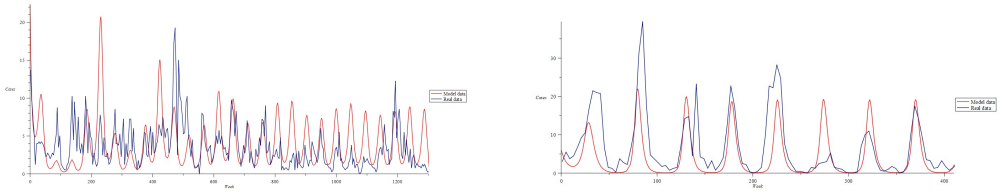

(a) Hepatitis A. (b) Sonne dysentery.

Figure 8: Dynamics of enteric infections.

The model reproduced the 4-year oscillation period of viral hepatitis A.

Frequency in Sonne dysentery was not revealed, since the ability of immunity to disappear suppresses oscillations. Only seasonal rises in incidence were observed.

4.5. Bloodborne and sexually transmitted infections

Weekly data on the number of new cases of gonorrhea was studied in Tula; monthly data on the number of new cases of viral hepatitis C and HIV infection was studied in Tula Region. The dynamics of the incidence of gonorrhea was studied from 1991 to 1996 (5 years), viral hepatitis C from 1991 to 2011 (20 years), and HIV infection from 1991 to 2021 (30 years).

The narcotic outbreak of hepatitis C, and the narcotic and sexual outbreak of HIV infection were analyzed. The average life expectancy of patients in the group with gonorrhea was 30 years; with hepatitis C and HIV infection, the average life expectancy of the group was 25 years with the narcotic transmission. The average lifetime of the group with HIV sexual transmission was 50 years. Sexual transmission of hepatitis C was not considered due to its low intensity Tahan et al. (2005).

The population involved in the active transmission amounted to 1,200 in gonorrhea and hepatitis C, and 2,000 in the HIV narcotic outbreak, and 14,000 in the sexual outbreak. The contagious period lasted 14 days for gonorrhea, 5 years for hepatitis C, and 2.5 years (the narcotic outbreak) and 6 years (the sexual outbreak) for HIV. With gonorrhea, re-infection is possible after 12 weeks, and after 10 years with hepatitis C (on average). With HIV infection, recovery is impossible, there is no immunity. HIV infection has the greatest susceptibility. The contact rate was 1.2 with gonorrhea, 2.7 with hepatitis C and 4.5 (the narcotic outbreak) and 1.5 (the sexual outbreak) with HIV. These infections suggest no seasonal prevalence.

Unlike HIV infection, with viral hepatitis C, there is both recovery and loss of immunity (variety of virus genotypes). Despite the mass infection during sexual intercourse, real and model data show that the narcotic transmission of hepatitis C and HIV infection remains significant.

Table 6: Parameters and initial conditions of the epidemic process of bloodborne infections and sexually transmitted infections.

	Gonorrhea	Viral hepatitis C	HIV infection (narcotic/sexual)
R	1.2	2.7	4.5/ 1.5
ι	0	0	0
θ	0	0	0
μ	0.000694	0.00333	0.00333/ 0.00167
k	0.07777	0.00833	0
α	0.5	0.01666	0.03/0.0138
β	0.5	0.001666	0
N	1,200	1,200	2,000/ 14,000
S_0	996	1,080	1,960
A_0	19	40	40
T	52.18	12	12
Dimension	Week	Month	Month

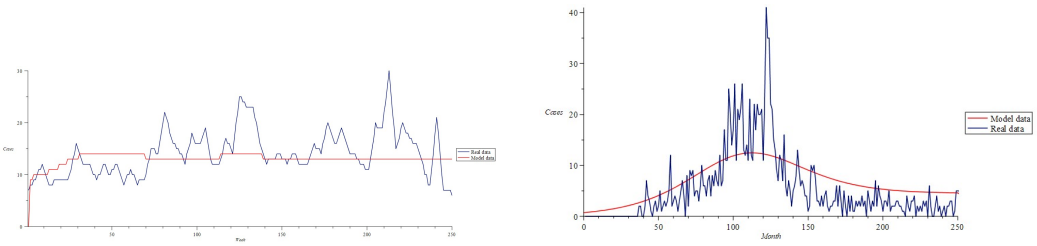

(a) Gonorrhea.

(b) Hepatitis C.

(c) HIV infection.

Figure 9: Dynamics of bloodborne infections and sexually transmitted infections.

There also was weekly data on the incidence of gonorrhea. The incidence was stable with occasional oscillations. The stability of the incidence is de-

termined by the virtual absence of immunity associated with the variability of *Neisseria gonorrhoeae*.

4.6. Comparative study of the dynamics of infections

According to the parameters of the infection process, infections were divided as follows: infections without immunity (HIV); infections with lifelong immunity (measles, mumps, chicken pox, whooping cough, viral hepatitis A); infections with possible loss of immunity, including due to the variability of microorganisms (rubella, scarlet fever, Sonne dysentery, gonorrhea, viral hepatitis C, influenza A, COVID-19). The model reproduces quantitative and qualitative characteristics, as well as the dynamics of these diseases. The study shows that the set of variables and parameters is necessary and sufficient.

The highest contact rate R was observed with COVID-19 (5.7), measles (5.1), narcotic spread of HIV infection (4.5), and influenza A (4.4); the lowest R was with gonorrhea (1.2), sexual spread of HIV (1.5), and scarlet fever (1.6). The contact rate range shows that the pathogens of these diseases are in a state of compromise with the human population Alizon et al. (2009).

The value of the contact rate R can vary depending on the type of transmission, with HIV infection being an excellent example van den Driessche (2017).

Interestingly, infections with a fecal-oral transmission mechanism (hepatitis A, Sonne dysentery) are similar to infections with an aerosol transmission (rubella, chicken pox). This confirms the paradigm of host-parasite interactions.

The greatest values of seasonal oscillations were found in chicken pox (0.45) and viral hepatitis A (0.40); this is associated with the effect of organized groups formed in kindergartens and schools.

The results of mathematical modeling have shown that the concept controlling model (with zero level of control) adequately reproduces the incidence dynamics.

In general, the model describes well the average, minimum, and maximum levels of incidence with matching peaks. Therefore, it can be assumed that it enables the reliable measurement of transmissibility and the reliable assessment of the intensity of the epidemic process. The known intensity allows an exact understanding of control.

Whooping-cough, influenza and respiratory streptococcal infection, scarlet fever show some lag in the coincidence of the incidence peaks, because the

increase in the incidence of these infections is partially mediated by genetic variability of the pathogen. The parameters of all the above infections are defined in the study, and are also given in Appendix A.

5. Use of the model to implement intervention campaigns

Thirteen intervention campaigns were analyzed, 11 of them for acute infections and 2 for chronic infections (HIV and viral hepatitis C). Ten intervention campaigns were implemented, the necessary resources and facilities were calculated additionally for 3 campaigns. (The material on infections is analyzed in the same order in which they were located in Section 4.1)

Necessary control forces were calculated by the formula and numerical solution of differential equations.

If there are no effective measures, it is the spontaneous development (SP). If the control measures only diminish incidence, this is the subcritical control (SC). If the epidemic process is interrupted, the control is effective (EF). If the campaign starts with the subcritical method (SC) and ends with effective method (EF) this method of control is called piecewise (PW).

5.1. Measles

The measles vaccination campaign began in 1968. Due to the high efficiency of the vaccine, only the vaccination campaign was supposed to be performed, without special measures to identify the sources of the infectious agent and reduce the mechanism of transmission. Calculation by formulas showed the critical level of vaccination λ_1 not less than 0.008168, the time of termination of the measles epidemic process T hould were 249 weeks. Vaccination was launched at a lower intensity, namely $\lambda_1 = 0.0079$, the time to achieve a reduction in incidence was 340 weeks, but after 360 weeks (from the start of the vaccination campaign) measles outbreaks intermittently occurred (subcritical control). In April 1976, up to 85 cases of diseases were registered per week, May 1982 up to 48 cases, and March 1984, October 1984, April 1985, June 1987, April 1988 up to 10-14 cases.

In 1994, the campaign was revised: the intensity of vaccination increased to critical ($\lambda_1 = 0.008168$). There was a particular focus on the immunization of individuals before entering kindergartens and schools. Since 1994, only a few cases were recorded: four in July 2003, one in August 2003, one in September 2003, one in October 2018, and seven in March 2019. Currently,

priority is given to revaccination of the elderly. The total follow-up was 60 years, from 1961 to 2021.

5.2. Mumps

The vaccination campaign began in 1982. Initial calculations showed the following parameters of the intervention campaign: $\lambda_1 = 0.00418$; $\delta_1 = 0.03$; $r = 0.2$; $T = 186$ weeks.

Since the calculations show an unsatisfactory long time to achieve the result, the volume of interventions was recalculated in order to reliably withdraw from the critical level towards efficiency. Taking into account the capabilities of the healthcare system, the level $T = 125$ weeks was chosen. Accordingly, the campaign indicators were: $\lambda_1 = 0.0086$; $\delta_1 = 0.03$; $r = 0.2$. With these parameters, the campaign proved effective.

From January to April 1999, there was an outbreak of mumps associated with the introduction of infection into the area.

5.3. Chicken pox

The chicken pox vaccine is not included in the national vaccination schedule in the Russian Federation. In this regard, a future intervention campaign was calculated. Taking into account certain activity of the chicken pox epidemic process, the following intervention campaign was developed: $\lambda_1 = 0.003625$; $\delta_1 = 0.02$; $r = 0.3$; $T = 102$ weeks and is pending realization.

5.4. Whooping cough

The vaccination campaign began in 1995. According to calculations, the intensity of vaccination λ_1 was 0.00565, $r = 0.2$; $\delta_1 = 0.03$; $T = 125$ weeks.

However, the indicated intensity of control parameters failed to be achieved. The whooping cough vaccine was not fully effective. Taking into account the efficacy of the vaccine, the actual vaccination intensity λ_1 equaled 0.005, and this vaccination intensity turned out to be below critical. The number of whooping cough cases decreased by 5 times: from 6-10 cases to 0-2 cases per week. Patients with whooping cough were actively identified, isolated and treated. Thus, whooping cough cases persist suggesting subcritical control.

The pathogen has antigenic variability and continues to circulate among both children and adult population, which is the cause of remaining incidence.

5.5. Rubella

As vaccines became available, an intervention campaign was planned to prevent the incidence of rubella since 2007. According to the plan, the intensity of vaccination λ_1 was to be 0.001694; intensity of detection and isolation of sources of infectious agents was planned as $\delta_1 = 0.05$. Sanitation measures in organized groups (increased requirements for intra-group isolation and ventilation of premises) were at $r = 0.4$. The time of termination of the epidemic process was to be $T = 73$ weeks.

The main planned indicators during the campaign were achieved. The actual vaccination rates were at $\lambda_1 = 0.0017$ upon reaching the planned level r and δ_1. The intervention campaign started on Week 1,550 (2007). The time to achieve the result was 92 weeks.

5.6. Scarlet fever

The epidemic process of scarlet fever was controlled simultaneously with the control of the epidemic process of streptococcal pharyngitis. The control parameters of the epidemic process of scarlet fever were determined as follows: $\lambda_1 = 0.0008$; $\delta_1 = 0.07$; $r = 0.15$; $T = 70$ weeks. Pre- and post-exposure prophylaxis with antibiotics was supposed to reduce susceptibility. However, these activities could not be implemented fully due to significant adverse events and treatment refusals. The intervention campaign began in 1984. Parameters of the conducted campaign were $\lambda_1 = 0.0006$; $\delta_1 = 0$; $r = 0$. The cases were not always timely detected, as at the time of detection patients had infected healthy individuals. The incidence of scarlet fever decreased by 4 times, but it remains 10 cases per week during the seasonal rise in October, a month after organized groups are formed in schools and kindergartens. The campaign showed subcritical control.

5.7. Influenza A

The parameters of influenza A epidemic process control were determined as follows: $\lambda_1 = 0.000429$; $\lambda_2 = 0.000035$; $\delta_1 = 0.03$; $r = 0$; $T = 260$ days. The planned time to achieve the result was 400 days. Seasonal vaccines were applied on the basis of the last strain of the previous seasonal period. Vaccinations were planned for both susceptible and recovered patients. The campaign started in 2004. It was possible to almost completely follow the parameters intended via the calculations. The actual time to reach the result was 600 days. The campaign can be considered effective, vaccination and revaccination against influenza continues annually.

5.8. COVID-19

The intervention campaign is given on the example of Moscow. The COVID-19 epidemic started with the following initial conditions 89 percent susceptibility, $A_0 = 200$ (the absolute number of patients). The contact rate R of the spread of the Wuhan variant at the start was 2.7. The population involved in active contact was 1 million.

The lockdown was announced on Day 68 of the epidemic, the intensity of the lockdown was $r = 1.62$. On the 195th day of the epidemic, a partial lockout occurred that lasted until Day 380 ($r = 0.945$). From Day 380 the lockout became complete ($r = 0$). The intensity of detection, isolation and treatment of sources of infection was $\delta_1 = 0.09$.

The lockdown saved time for the deployment of beds, including intensive care units, to ensure a reduction in COVID-19-related fatalities. Type of the control appeared to be piecewise.

5.9. Viral hepatitis A

Viral hepatitis A was a serious problem for the area (Novomoskovsk, Tula Region) through the unsatisfactory sanitary and hygienic condition of the water supply in certain parts of the city, which triggered a seasonal epidemic. Further, the epidemic was actively supported by contact and community-acquired transmission of the virus (person to person transmission) in schools and pre-schools. An intervention campaign was planned with a focus on the transmission mechanism, $r = 1$. Other parameters of the intervention campaign were $\lambda_1 = 0.001146$; $\lambda_2 = 0$; $\delta_1 = 0.05$; $T = 96$.

The campaign started in 1997. The water supply was reconstructed and group isolation and disinfection measures were introduced in organized groups in schools and pre-schools, as well as vaccination of children and adults. The actual campaign parameters: $\lambda_1 = 0.00047$; $\lambda_2 = 0$; $\delta_1 = 0.26$; $r = 0.5$. The time to achieve the result was 450 weeks. The campaign can be considered effective.

5.10. Sonne dysentery

The epidemiological significance of Sonne dysentery was defined by the intensive contact and community-acquired transmission in schools and preschools between 1991 and 1999. An intervention campaign was planned with an emphasis on the reconstruction of preschool institutions with the introduction

of intra-group isolation, as well as provision of more kindergartens. The regulations for medical personnel at schools and preschool institutions for the identification of symptoms and laboratory tests were introduced.

The campaign started in 1999. Planned indicators were $\lambda_1 = 0$; $\lambda_2 = 0$; $\delta_1 = 0.09$; $r = 1.497$; $T = 26$ weeks. Identified and diseased individuals were isolated, treated and returned to the population both susceptible and non-susceptible.

The actual campaign indicators were $\lambda_1 = 0$; $\lambda_2 = 0$; $\delta_1 = 0.09$; $r = 1.05$. The result was achieved 40 weeks after the launch of the intervention campaign. The campaign can be considered effective.

5.11. Gonorrhea

An intervention campaign with a critical impact level for this disease was not planned. The control efforts of two stages of the current anti-epidemic measures (1996 to 2004, 2004 to 2022) were evaluated. In 1996-2004, there was a decrease in transmission through the use of condoms $r = 0.06$, detection and treatment with training in safe behavior with an intensity of $\delta_2 = 0.1$. In 2004-2022, the intensity of these activities was $r = 0.12$; $\delta_1 = 0.118$. The interventions showed the piecewise control.

5.12. Viral hepatitis C

A population of injecting drug users with a total of 1,200 people was considered. Calculations for the critical levels showed a longer duration of achievement of the result. Therefore, enhanced parameters of the intervention campaign were planned: $\lambda_1 = 0.02$; $\lambda_2 = 0.02$; $\delta_1 = 0.06$; $r = 1$; $T = 99$ months. The indicator λ_1 denoted pre-exposure prophylaxis with sofosbuvir in susceptible patients, λ_2 was pre-exposure prophylaxis with sofosbuvir in recovered and treated patients, δ_1 was detection and treatment. The campaign is planned after direct acting agents and sofosbuvir for pre-exposure prophylaxis are made available. Measures to counteract/ensure the safety of injecting drug use are also planned Kretzschmar and Wiessing (2008).

5.13. HIV infection

A population of injecting drug users with a total of 2,000 people was considered. After the narcotic outbreak, that happened in 2000, program of screening and treatment was implemented with intensity $\delta_1 = 0.01$. The critical levels of control in HIV infection were determined as $\lambda_1 = 0.015$; $\lambda_2 = 0$; $\delta_1 = 0.06$; $r = 0.155$; $T = 143$ months. The parameter r is the

impact on the mechanism of infection transmission (injecting drug use), δ_1 is the identification of sources of the infectious agent with taking for treatment and removal from the population, as it is assumed that the same number of new injecting drug users replaces those removed. The parameter δ_2 is detection and taking for treatment with remaining in the same group of injecting drug users. The parameter λ_1 is pre-exposure prophylaxis with antiretroviral drugs (tenofovir and emtricitabine, as well as other permitted drug combinations). COVID-19 postponed the beginning of the program. The program needs accumulation of the necessary resources and facilities, namely non-invasive tests for HIV infection, outreach workers for testing, and low-threshold access points for dispensing therapy.

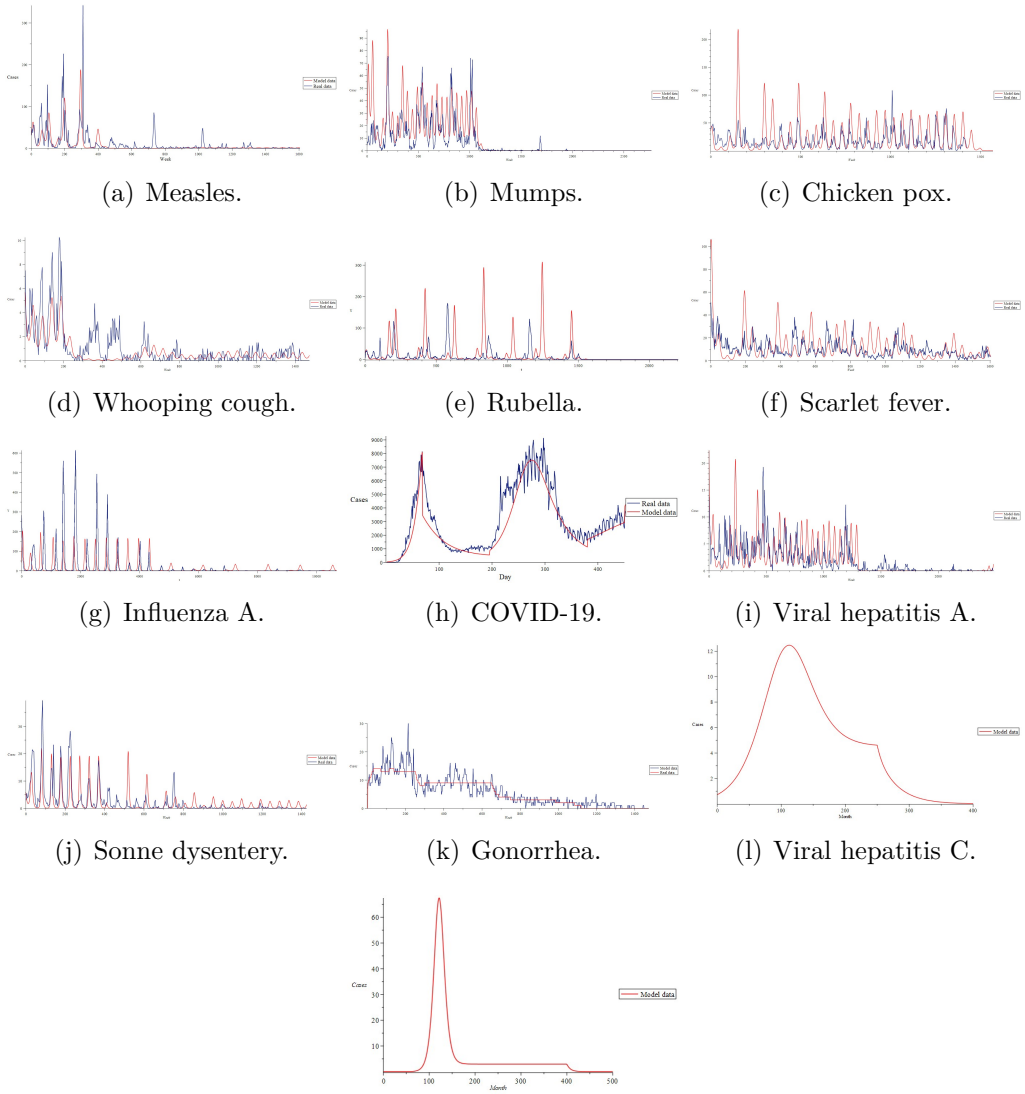

(a) Measles. (b) Mumps. (c) Chicken pox.

(d) Whooping cough. (e) Rubella. (f) Scarlet fever.

(g) Influenza A. (h) COVID-19. (i) Viral hepatitis A.

(j) Sonne dysentery. (k) Gonorrhea. (l) Viral hepatitis C.

(m) HIV infection.

Figure 10: Dynamics of the incidence of infections (a-m) in the setting of intervention campaigns from 1968 to 2021: comparison of model data with real data.

Table 7: Control parameters for contagious disease spectrum.

Parameter	Measles	Mumps	Chicken pox	Whooping cough	Rubella	Scarlet fever	Influenza A	COVID-19	Viral hepatitis A	Sonne dysentery	Gonorrhea	Viral hepatitis C	HIV infection
Estimated control parameters													
r	0	0.20	0.30	0.20	0.40	0.15	0	-	1.00	1.50	-	1.00	0.16
δ	0	0.03	0.02	0.03	0.05	0.07	0.03	-	0.05	0.12	-	0.06	0.06
λ	0.0082	0.0086	0.0036	0.0057	0.0017	0.0008	0.0004	-	0.0011	0	-	0.02	0.015
T_n	310	155	165	210	80	90	400	-	105	28	-	110	150
T_f	249	125	102	125	73	70	260	-	96	26	-	99	143
Dimension	52.18	52.18	52.18	52.18	52.18	52.18	365.25	-	52.18	52.18	-	12	12
Actual control parameters													
r	0	0.2	-	0	0.4	0	0	1.62/* 0.95/0	0.1	0.6	0.06/* 0.12	-	-
δ	0	0.03	-	0	0.05	0	0	0.5	0.26	0.4	0.1/0.118	-	-
λ	0.0082	0.0040	-	0.0035	0.0017	0.0006	0.0015	0	0.0005	0	0	-	-
T	340	630	-	-	92	-	600	-	450	40	-	-	-
Dimension	52.18	52.18	-		52.18	52.18	365.25	365.25	52.18	52.18	52.18	-	-
Type of control	EF	EF	SP	SC	EF	SC	EF	PW	EF	EF	PW	SP	SP

*Durations of the piecewise linear control phases are given in Sections 5.8 COVID-19 and 5.11 Gonorrhea.

6. Comparison of systems with sufficient and limited control resources

We compared variants of deliberatly simplified concept controlling model

- General variant
  $X' = -R\alpha XY + \mu - \mu X - \lambda X^{p_1}$
  $Y' = R\alpha XY - \beta Y - \mu Y - \delta Y^{p_2}$

- Mode1 $p_1 = p_2 = 1$
  $X' = -R\alpha XY + \mu - \mu X - \lambda X$
  $Y' = R\alpha XY - \beta Y - \mu Y - \delta Y$

- Model2 $p_1 = p_2 = 0$
  $X' = -R\alpha XY + \mu - \mu X - \lambda$
  $Y' = R\alpha XY - \beta Y - \mu Y - \delta$

where X is the proportion of susceptible individuals, Y is the proportion of infected (uncontrolled sources of infection), R is the contact rate, α is the intensity of infectiousness, β is the intensity of recovery, μ is the intensity of the natural movement of the population (birth and death rates, inflow and outflow), δ is the intensity of detection and taking for treatment of sources of infection, p_2 is the δ value of resources sufficiency, λ is the intensity of vaccination, p_1 is the λ value of resources sufficiency. Parameter values as of acute infection: $\alpha = \beta = 0.074$ (1/day), $R = 2$, $\mu = 0.000157$ (1/day), $\lambda = 0.00001$ (individuals/population).

In Model 1 (proportionate sufficient resources) the trace (tr) of the Jacoby matrix (J) of the nontrivial equilibrium (NTE) is always below zero, which means the system is either in a steady state or unstable with the hard loss of stability while traveling to the trivial equilibrium (TE). In figures dash is unstable equilibrium, solid is stable equilibrium - Fig. 11.

$$\mathrm{tr}(\mathrm{J}(\mathrm{System1})) = -\frac{\mu R\alpha}{\mu + \beta + \beta}$$

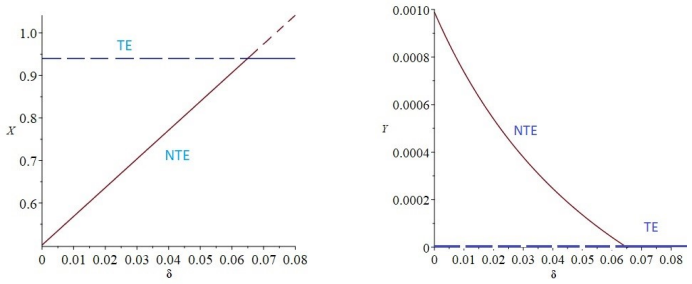

Figure 11: Bifurcation diagram of system 1 showing control evolution in direction enhancing force δ: X – left, Y – right.

In System 2 (unproportionate insufficient resources) the trace of the Jacoby matrix can be either above or below zero that completely changes the system behavior. With the growth of δ system passes the unstable cycle, mild loss of stability (with oscillations), hard loss of stability (without oscillations).

$$\begin{aligned}\mathrm{tr}(\mathrm{J}(\mathrm{System2})) = -\big[(-\mu+\delta+\lambda)R^2(\mu-\delta-\lambda)^2\alpha^2 - 2R\mu(\mu+\delta-\lambda)(\beta+\mu)\alpha + \\ + \mu^2(\beta+\mu)^2\big]^{1/2} - \mu^3 + (R\alpha-\beta-3\delta+\lambda)\mu^2 + \\ + \left(-2R(\delta+\lambda)\alpha - 5\left(\delta-\frac{\lambda}{5}\right)\beta\mu + R(\delta+\lambda)^2\alpha - 2\beta^2\delta\right)R\alpha\cdot \\ \cdot\left\{(\beta+\mu)\Big[-\mu^2+(R\alpha-\beta)\mu - R(\delta+\lambda)\alpha - \Big\{R^2(\mu-\delta-\lambda)^2\alpha^2 - \right. \\ \left. - 2R\mu(\mu+\delta-\lambda)\left[\beta+\mu+\mu^2(\beta+\mu)^2\right]^{1/2}\Big\}\Big]\right\}^{-1}\end{aligned}$$

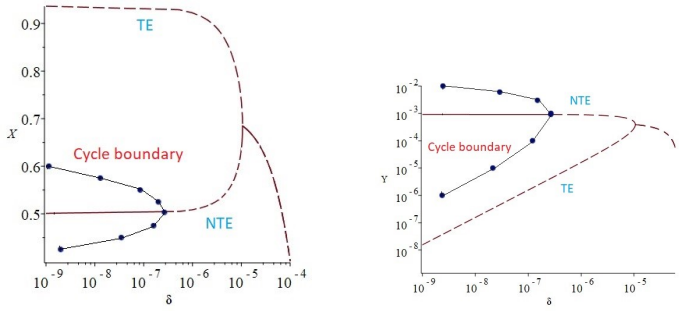

Figure 12: Bifurcation diagram of unproportionate system 2 showing control evolution in direction enhancing force δ: X – left, Y – right.

Aims of the epidemic control are only reached through hard loss of stability.

In sufficient control resources the system is plane and the hard loss of stability occurs after reaching the threshold. In limited resources the system behavior becomes complex and big oscillations may cause bifurcation to the end of the epidemic process.

Note 5. *In a system with limited resources, the trace of the Jacobi matrix can be both negative and positive, which means that with limited resources for identifying sources of the infectious agent, the system can lose stability with oscillations. Unstable cycles may occur. Such buildups are known in dynamical systems and are unfavorable for controlling.*

Note 6. *In conditions of limited resources, parametric portraits show areas of stability, instability with oscillations, instability without oscillations, depending on the level of control actions.*

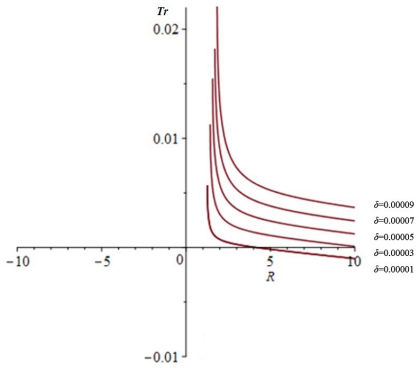

Figure 13: Dependence of the trace tr on the contact rate R at different levels of detection and treatment of sources of the infectious agent δ. $\mu = 0.00157$; $R = 3$; $k = 0$; $\lambda = 0.0001$; $\alpha = \beta = 0.074$.

When resources are limited, especially in rapid (acute) infections, constant (unproportionate) detection and treatment of pathogen sources can be accompanied by repeated outbreaks, which may severely hamper an intervention campaign - Fig. 12, 13.

7. Discussion and perspectives of the study

Determining the parameters of the epidemic process based on incidence data is an inverse problem, the formulation of conceptual models of epidemics and their control is the ill-posed problem Kabanikhin and Krivorot'ko (2020). For all studied diseases, the concept controlling model enabled the determination of the parameters of the epidemic process and control parameters. The formula for determining condition of arresting epidemics was operational. The formula values turned out to be comparable with the numerical solutions of the system of differential equations.

The concept controlling model enables the qualitative prediction of the movement of incidence, the time of peaks and declines, seasonal prevalence and frequency. It describes the qualitative behavior of the system: the presence or absence of oscillations in incidence, frequency of oscillations. The periodic rises of incidence are due to a combination of seasonal forcing and the natural frequency of the system's oscillations. The seasonal and periodic rises of the model data with the real data coincide; however, lead and lag of 5-6 weeks are possible. Our model is close to SEIR-HCD model Krivorot'ko et al. (2020).

In the work we found, that several control options are possible, whether effective or not, options shown in Table 8

Table 8: Options for controlling the epidemic process.

Control Option	Graph	Explanation
Option 1. Spontaneous development of the epidemic SP	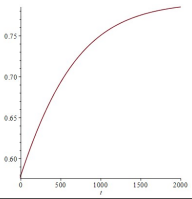	The solution of the differential equations is an increasing function with saturation, no control.
Option 2. Inefficient control NE with increasing incidence	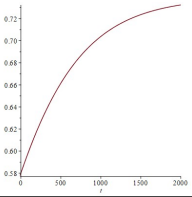	The solution is an increasing function with saturation at a slightly lower level than with no exposure.
Option 3. Sub-critical control SC with a decrease in incidence	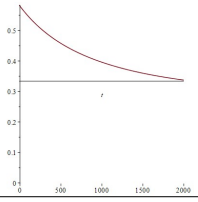	The solution is a decreasing function that reaches lower values but never reaches the target value.
Option 4. Effective control EF with the elimination of infection	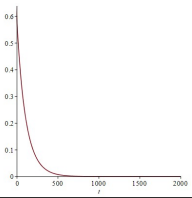	The solution is a control curve, a decreasing function that reaches the values of the no infection after time T
Option 5. Control in a piece-wise linear mode PW with the elimination of infection	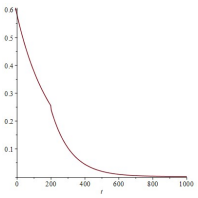	A phasing is recommended with increased control at subsequent phases (acceleration of the active search for cases as their number decreases). The first 600 days, Mode 3 is applied; in the next 600 days Mode 4 is applied with the elimination of the incidence in the area.

In the absence of control - spontaneous development of the disease, the

incidence inexorably increases reaching saturation at a very high level (Option 1). Inefficient control (Option 2) and sub-critical control (Option 3) are far from the aim of arresting the epidemic. Upon reaching the required levels of exposure, a phase transition to the elimination of infection is performed (Option 4). Piece-wise linear control is possible, where a milder mode is applied at the first stages, and a harder ("cleaning") mode is used at subsequent stages (Option 5). This approach allows saving resources at the first stages of the intervention campaign with the avoided prolonged attainment of the target result at subsequent stages.

Rule 2. *It is recommended that the search for cases be intensified as the intervention campaign advances.*

Of the 10 intervention campaigns that took place, 6 proved effective (EF), 2 were sub-critical (SC). In 2 cases, a piece wise approach to changing the parameters was applied (PW). In 3 cases, spontaneous development of the process (SP) was observed (measures are planned).

The actual duration of intervention campaigns sometimes happened to be longer than predicted. This is due to oscillations in control efforts and a temporary shortage of resources and/or facilities.

It is necessary to solve two fundamental questions: how the sinusoidal forcing (question 1) and random oscillations (question 2) affect the model and the formula. Additional research is required.

The value of contact rate R may vary not only within the nosology, but also depending on the territory, population groups and time-frame. A good example is HIV showing high contact rate in narcotic users and relatively low contact rate in heterosexual transmission. The parameter R depends on the strain variability: the value of R in Delta variant is lower than in the Omicron variant.

The model is applied for binary (two-term) parasitic systems, infectious-immunological relations between the parasite and the host. More complex models are used for tripartite parasitic systems that include vectors, as well as for diseases with a long persistence of the pathogen in the environment.

A varying profile of model parameters enables the prediction of the dynamics of both acute and chronic infections, both infections with aerosol and fecal-oral transmission mechanisms, although the epidemiology of these infections is fundamentally different.

New and recurring infections are encountered by field epidemiologists who use personal computers and are not equipped with supercomputers.

Therefore, simple models that do not require resource-intensive hardware are of particular importance. The epidemic process control formula is powerful resource and can be implemented arithmetically and on all devices without limitation. We regard it as the necessary control tool.

Mutual potentiation of anti-epidemic measures of different directions is extremely important. With successful identification, isolation and treatment of patients, as well as vaccination, the size of lockdown (that is economically destructive) can be reduced. Freedom of choice suggests that work can be less intensive and the result will be obtained after a longer period of time, or the labour can be more intense and the result will come faster. Similarly to bank loans, often a quick repayment is cheaper, but we have to deal with time-based budgeting.

Piece-wise linear controlling is suggested for this paper. We start with the mild control - noncritical fall of incidence. Then we pass to the enhanced control with critical fail of incidence (that is above threshold and allows elimination). It is evident that on the first step sub-critical control is easy to be organised but it provides the fertilized soil for more intense finishing action. Thus arresting epidemics occurs.

We also show that that epidemic process control at limited resources in acute infections may be dangerous due to oscillations.

Of particular interest are system trajectories, and epidemiological corridors (tunnels), when moving through which the epidemic process is interrupted.

The mechanism for adjusting the planned and actual (current) control trajectory is subject to further study that involves the determination of a need for it to be corrected in case of deviation from the specified trajectory due to insufficient resources (or poor activity) or inaccurately defined parameters. This also applies to a group of ill-posed problems. It seems particularly relevant to improve methods for determining the parameters of an epidemic process based on their measurement by really robust methods (the inverse problem).

8. Conclusion

We briefly reviewed the types of mathematical models of epidemics. Next, we chose essential parameters of the infectious and epidemic process, necessary and sufficient for epidemic control tool, aimed on arresting epidemics.

The concept controlling model qualitatively and quantitatively describes the system behavior.

The spectrum of pathogens and infectious diseases used to be defined by the following parameters: the intensity of infection and recovery, the rate of loss of immunity and the intensity of the inflow/outflow of the population, death rate. There are three control coefficients: r, security and restrictive measures; δ, identification, isolation and treatment of sources of infection; λ, vaccination, the last two exist in the two variants described above.

We define three targets of controlling: infected persons (detection, isolation and treatment δ), the mechanism of transmission (security and restrictive measures, sanitation activities r), as well as susceptibility reduction (vaccination, pre- and post-exposure prophylaxis λ).

Concept controlling model is sharpened to plan intervention campaign and check its efficacy. The epidemic control tool presented in the paper identifies conditions to achieve the elimination and evaluate time to elimination. Below formula levels intervention measures are ineffective.

Control measures enhance each other. The greater the influence of vaccination and pre-exposure prophylaxis and the more intensive the identification and restriction of sources of the infectious agent, the less amount of lockdown is needed. The higher the level of vaccination and pre-exposure prophylaxis, the lower can be be the level of detection of sources of the infectious agent. If all measures are aggressive, time to elimination is reduced. Epidemiological diagrams are suggested, that allows to combine directions of controlling and time perfectly.

This paper demonstrates the efficacy of the concept controlling model with regard to real data and the potential of using epidemic control tool to plan the intervention and check its efficacy.

It is assumed that each area should be certified according to the main demographic characteristics and the number of risk groups, and basic models of actual infections and long-term plans for their elimination should be in place. If this is done, the readiness for both new and recurring diseases is higher.

In conditions of limited resources, parametric portraits show areas of stability, instability with oscillations, instability without oscillations, depending on the level of control actions.

To sum it up, mathematical modeling of the epidemic process is an effective tool in the elimination of disease incidence. The concept controlling model provides a useful framework to study the specifics of epidemic process

and estimate the level of control measures.

9. Funding

This work was carried out with the financial support of the Ministry of Education and Science of the Russian Federation: grant No. 075-11-2020-011 (13.1902.21.0040).

Appendix A. Parameters of the infection process of acute and chronic infections

Chronic infections

	Disease	Infection rate α	Recovery rate β (1/days)	Source	Immunity loss rate k (1/days)	Source
1	HIV infection	0.00046019	0	Williams et al. (2011)	0	Drain et al. (2019)
2	Viral hepatitis C	0.00055533	0.000055	Aitken et al. (2008)	0.00027767	Currie et al. (2008)

Acute infections

	Disease	Infection rate α and recovery rate β (1/days)	Source	Immunity loss rate k (1/days)	Source
3	Chicken pox	0.04714286	Freer and Pistello (2008)	0	Gershon and Gershon (2013)
4	Viral hepatitis A	0.03571429	Czumbel et al. (2018)	0	Hussain et al. (2006)
5	Influenza	0.2	Cori et al. (2012)	0.00005	Woolthuis et al. (2017)
6	Gonorrhea	0.071429	Hethcote et al. (1982)	0.01111	Russell et al. (2020)
7	Sonne dysentery	0.1	Shad and Shad (2021)	0.00285714	Allen et al. (2021)
11	Whooping cough	0.05262857	Pesco et al. (2014)	0	Rozhnova and Nunes (2012)
12	Measles	0.09	Finkenstädt et al. (2002)	0	Corey and Noymer (2016)
13	Rubella	0.05257	Edmunds et al. (2000)	0.00003586	Yang and Silveira (1998)
20	Respiratory streptococcal infection, scarlet fever	0.142857	Basetti et al. (2017)	0.00005476	Zhong and Wang (2020)
24	Mumps	0.04542857	Anderson et al. (1987)	0	Greenhalgh (1988)
26	New coronavirus infection COVID-19	0.074	Singanayagam et al. (2020); Puhach et al. (2022)	0.0055	Cherednik (2021); Inthamoussou et al. (2022)

For acute infections $\alpha = \beta$

Appendix B. Derivation of the formula for arresting epidemics

To derive the formula for arresting epidemics we make several assumptions during arresting period. We 1) neglect the death rate, 2) do not form quarantine class Q - revealed infected are treated and move directly to resistant class R, 3) vaccinated people carefully re-vaccinate and confirm their vaccine immunity, 4) fore simplification purposes instead of three classes (E - exposed, A - acute infected, C - chronically infected) one class I is formed,

5) sum of all classes is equal to 1 ($S + I + R + V = 1$), thus calculation of classes is available in proportion.

The assumption system comprises 3 independent differential equations for classes S, I and R and dependant differential equation for class V:

$$\begin{cases} S(t)' = -R\alpha S(t)I(t) + \mu - \mu S(t) + kR(t) - \lambda S(t) \\ I(t)' = R\alpha S(t)I(t) - (\beta + \mu + \delta)I(t) \\ R(t)' = (\beta + \delta)I(t) - (k + \mu)R(t) \\ V(t)' = \lambda S(t) - \mu V(t) \end{cases} \tag{B.1}$$

Assume the approximate solution $I(t) = I_0$, then the differential equation for $R(t)$ is written as

$$\frac{d}{dt}R(t) = (\beta I_0 + \delta) - (k + \mu)R(t)$$

We solve this differential equation and assume $R_0 = 1 - X_0 - Y_0$

$$R(t) = \frac{((-k - \mu - \beta - \delta - \lambda)I_0 - (S_0 - 1)(k + \lambda + \mu))e^{-(k+\lambda+\mu)t} + (\beta + \delta)I_0}{k + \lambda + \mu}$$

Insert expression for R(t) into the differential equation for S(t) and solve it

$$\begin{aligned} &S(t) = (\frac{1}{(k + \lambda + \mu)(RI_0\alpha - k)(RI_0\alpha + \lambda + \mu)} \\ &(k + \lambda + \mu)((RI_0^2\alpha + (-R\alpha + \beta + \delta + \lambda + \mu)I_0 - \lambda)k + \\ &+ I_0\alpha R(RS_0I_0\alpha + (X_0 - 1)mu + X_0\lambda))e^{-(R\alpha I_0+\lambda+mu)t} - \\ &- k((S_0 + I_0 - 1)k + (\lambda + \mu + \beta + \delta)I_0 + (S_0 - 1)(\lambda + \mu))(R\alpha I_0 + \lambda + \mu) \\ &e^{-(k+\lambda+\mu)t} + (R\alpha I_0 - k)(((\beta + \delta)I_0 + \mu)k + \mu(\lambda + \mu)) \end{aligned}$$

Insert expression for S(t) into the differential equation for I(t) and solve it. Obtaining

$$Y(t) = Ae^{\frac{B}{((k+\lambda+\mu)^2(RI_0\alpha+\lambda+\mu)^2(RI_0\alpha-k)))}}$$

where

$$\begin{aligned} &A = -(\frac{1}{(k + \lambda + \mu)^2(RI_0\alpha + \lambda + \mu)^2} \\ &((RI_0^2\alpha + (-R\alpha + \beta + \delta + \lambda + \mu)I_0 - \lambda)k^2 + \\ &+ (R\alpha(\lambda + \mu + \beta + \delta)I_0^2 - (\lambda + \mu)(-\lambda - \mu + (S_0 + 1)R\alpha - 2\beta - 2\delta)I_0 - \\ &(\lambda + \mu)((S_0 + 1)\lambda + (S_0 - 1)\mu))k \end{aligned}$$

$$B = -(k+\lambda+\mu)^2\alpha R(R^2 S_0 I_0^2 \alpha^2 + I_0((I_0-1)k + (S_0-1)\mu + S_0\lambda)R\alpha + k((\lambda+\mu+\beta+\delta)I_0 -$$
$$- \lambda))e^{-(RI_0\alpha+\lambda+\mu)t} - (-k\alpha R((S_0+I_0-1)k + (\lambda+\mu+\beta+\delta)I_0 +$$
$$+ (S_0-1)(\lambda+\mu))(R\alpha I_0 + \lambda + \mu)e^{-(k+\lambda+\mu)t} +$$
$$+ (k+\lambda+\mu)(R\alpha I_0 - k)t((\mu(I_0-1)k + (\lambda+\mu)((\mu+\beta+\delta)I_0 - \mu))$$
$$R\alpha + (\mu+\beta+\delta)(\lambda+\mu)(k+\lambda+\mu)))(R\alpha I_0 + \lambda + \mu)$$

From this equation applying simplification we get Formula 2.

References

Aitken, C.K., Lewis, J., Tracy, S. L. Spelman, T., Bowden, D. S. Bharadwaj, M., Drummer, H., Hellard, M., 2008. High incidence of hepatitis C virus reinfection in a cohort of injecting drug users. Hepatology 48, 1746–1752. doi:10.1002/hep.22534.

Alizon, S., Hurford, A., Mideo, N., Van Baalen, M., 2009. Virulence evolution and the trade-off hypothesis: history, current state of affairs and the future. Journal of Evolutionary Biology 22, 245–259. doi:10.1111/j.1420-9101.2008.01658.x.

Alizon, S., van Baalen, M., 2005. Emergence of a convex trade-off between transmission and virulence. The American Naturalist 165, 155–167. doi:10.1086/430053.

Allen, H., Mitchell, H.D., Simms, I., Baker, K.S., Foster, K., Hughes, G., Dallman, T., Jenkins, C., 2021. Evidence for re-infection and persistent carriage of Shigella species in adult males reporting domestically acquired infection in england. Clinical Microbiology and Infection 27, 126.e7–126.e13. doi:10.1016/j.cmi.2020.03.036.

Anderson, R., 1982. Transmission dynamics and control of infectious disease agents, in: Population Biology of Infectious Diseases, pp. 149–176.

Anderson, R., 2013. The population dynamics of infectious diseases: theory and applications. Springer.

Anderson, R., Fraser, C., Ghani, A., Donnelly, C., Riley, S., Ferguson, N., Leung, G., Lam, T., Hedley, A., 2004. Epidemiology, transmission dynamics and control of sars: the 2002–2003 epidemic. Philosophical Transactions of the Royal Society A 359, 1091–1105. doi:10.1098/rstb.2004.1490.

Anderson, R., May, R., 1992. Infectious diseases of humans: dynamics and control. Oxford university press.

Anderson, R.M., Crombie, J.A., Grenfell, B.T., 1987. The epidemiology of mumps in the uk: A preliminary study of virus transmission, herd immunity and the potential impact of immunization. Epidemiology and Infection 99, 65–84. doi:10.1017/S0950268800066875.

Arifin, S., Zimmer, C., Trotter, C., Colombini, A., Sidikou, F., LaForce, F., Cohen, T., Yaesoubi, R., 2019. Cost-effectiveness of alternative uses of polyvalent meningococcal vaccines in niger: An agent-based transmission modeling study. Med Decis Making 39, 553–567. doi:10.1177/0272989X19859899.

Aronna, M., Guglielmi, R., Moschen, L., 2021. A model for covid-19 with isolation, quarantine and testing as control measures. Epidemics 34, 100437. doi:10.1016/j.epidem.2021.100437.

Atkins, K., Read, A., Walkden-Brown, S., Savill, N., Woolhouse, M., 2013. The effectiveness of mass vaccination on marek's disease virus (mdv) outbreaks and detection within a broiler barn: A modeling study. Epidemics 5, 208–217. doi:10.1016/j.epidem.2013.10.001.

Basetti, S., Hodgson, J., Rawson, T., Majeed, A., 2017. Scarlet fever: a guide for general practitioners. London Journal of Primary Care 9, 77–79. doi:10.1080/17571472.2017.1365677.

Beliakov, V., 1974. Revoliutsiia v epidemiologii. Zhurnal Mikrobiologii Epidemiologii i Immunobiologii 12, 20–24.

Benenson, A., 1981. Control of communicable diseases in man. American Public Health Association.

Bensoussan, A., Frehse, J., Yam, P., 2013. Mean Field Games and Mean Field Type Control Theory. Springer, New York. doi:10.1007/978-1-4614-8508-7.

Biggerstaff, M., Cowling, B., Cucunubá, Z., Dinh, L., Ferguson, N., Gao, H., Hill, V., Imai, N., Johansson, M., Kada, S., Morgan, O., Pastore, Y., Piontti, A., Polonsky, J., Prasad, P., Quandelacy, T., Rambaut, A., Tappero, J., Vandemaele, K., Vespignani, A., Warmbrod, K., Wong, J., 2020. Early insights from statistical and mathematical modeling of key epidemiologic parameters of covid-19. Emerging Infectious Diseases 26, e1–e14. doi:10.3201/eid2611.201074.

Brauer, F., Castillo-Chavez, C. and, F.Z., 2019. Mathematical Models in Epidemiology. Springer-Verlag.

Cano, C., 2020. The SIR Models, their Applications, and Approximations of their Rates. Technical Report. Louisiana Tech University.

Cauchemez, S., Ferguson, N., 2008. Likelihood-based estimation of continuous-time epidemic models from time-series data: Application to measles transmission in london. Journal of The Royal Society Interface 5, 885–897. doi:10.1098/rsif.2007.1292.

Cevik, M., Tate, M., Lloyd, O., Maraolo, A., Schafers, J., 2021. Sars-cov-2, sars-cov, and mers-cov viral load dynamics, duration of viral shedding, and infectiousness: a systematic review and meta-analysis. Lancet Microbe 2, e13–e22. doi:10.1016/S2666-5247(20)30172-5.

Chen-Charpentier, B., Stanescu, D., 2010. Epidemic models with random coefficients. Mathematical and Computer Modelling 52, 1004–1010. doi:10.1016/j.mcm.2010.01.014.

Cherednik, I., 2021. Modeling the waves of covid-19. Acta Biotheoretica 70, 1–36. doi:10.1007/s10441-021-09428-w.

Cherry, J.D., 2013. Pertussis: challenges today and for the future. PLOS Pathogens 9, e1003418. doi:10.1371/journal.ppat.1003418.

Corey, K.C., Noymer, A., 2016. A "post-honeymoon" measles epidemic in burundi: mathematical model-based analysis and implications for vaccination timing. PeerJ 4, 1–22. doi:10.7717/peerj.2476.

Cori, A., Valleron, A.J., Carrat, F., Scalia Tomba, G., Thomas, G., Boëlle, P.Y., 2012. Estimating influenza latency and infectious period durations using viral excretion data. Epidemics 4, 132–138. doi:10.1016/j.epidem.2012.06.001.

Currie, S.L., Ryan, J.C., Tracy, D., Wright, T.L., George, S., McQuaid, R., Kim, M., Shen, H., Monto, M., 2008. A prospective study to examine persistent HCV reinfection in injection drug users who have previously cleared the virus. Drug and Alcohol Dependence 93, 148–154. doi:10.1016/j.drugalcdep.2007.09.011.

Cutts, F., Dansereau, E., Ferrari, M., Hanson, M., McCarthy, K., Metcalf, C., Takahashi, S., Tatem, A., Thakkar, N., Truelove, S., Utazi, E., Wesolowski, A., Winter, A., 2020. Using models to shape

measles control and elimination strategies in low- and middle-income countries: A review of recent applications. Vaccine 38, 979–992. doi:10.1016/j.vaccine.2019.11.020.

Czumbel, I., Quinten, C., Lopalco, P., Semenza, J.C., ECDC expert panel working group, 2018. Management and control of communicable diseases in schools and other child care settings: systematic review on the incubation period and period of infectiousness. BMC Infectious Diseases 18, 199. doi:10.1186/s12879-018-3095-8.

Datta, A., Winkelstein, P., Sen, S., 2022. An agent-based model of spread of a pandemic with validation using covid-19 data from new york state. Physica A: Statistical Mechanics and its Applications 585, 126401. doi:10.1016/j.physa.2021.126401.

Demongeot, J., Griette, Q., Magal, P., 2020. Si epidemic model applied to covid-19 data in mainland china. Royal Society Open Science 7, 201878. doi:10.1098/rsos.201878.

Drain, P.K., Dorward, J., Bender, A., Lillis, L., Marinucci, F., Sacks, J., Bershteyn, A., Boyle, D.S., Posner, J.D., Garrett, N., 2019. Point-of-care HIV viral load testing: an essential tool for a sustainable global HIV/AIDS response. Clinical Microbiology Reviews 32, e00097–18. doi:10.1128/CMR.00097-18.

van den Driessche, P., 2017. Reproduction numbers of infectious disease models. Infectious Disease Modelling 2, 288–303. doi:10.1016/j.idm.2017.06.002.

Edmunds, W.J., van de Heijden, O.G., Eerola, M., Gay, N.J., 2000. Modelling rubella in europe. Epidemiology & Infection 125, 617–634. doi:10.1017/s0950268800004660.

Fazakas-Anca, I.S., Modrea, A., Vlase, S., 2021. Using the stochastic gradient descent optimization algorithm on estimating of reactivity ratios. Materials (Basel) 14, 4764. doi:10.3390/ma14164764.

Ferguson, N., Laydon, D., Nedjati Gilani, G., Imai, N., Ainslie, K., Baguelin, M., Bhatia, S., Boonyasiri, A., Cucunuba Perez, Z., Cuomo-Dannenburg, G., Dighe, A., Dorigatti, I., Fu, H., Gaythorpe, K., Green, W., Hamlet, A., Hinsley, W., Okell, L., Van Elsland, S., Thompson, H., Verity,

R., Volz, E., Wang, H., Wang, Y., Walker, P., Walters, C., Winskill, P., Whittaker, C., Donnelly, C., Riley, S., Ghani, A., 2020. Report 9: Impact of non-pharmaceutical interventions (NPIs) to reduce COVID19 mortality and healthcare demand. Technical Report. Imperial College London. doi:10.25561/77482.

Ferretti, L., Wymant, C., Kendall, M., Zhao, L., Nurtay, A., Abeler-Dörner, L., Parker, M., Bonsall, D., Fraser, C., 2020. Quantifying sars-cov-2 transmission suggests epidemic control with digital contact tracing. Science 368, eabb6936. doi:10.1126/science.abb6936.

Feßler, R., 2020. A General Integral Equation Model for Epidemics. Technical Report. Fraunhofer Institute for Industrial Mathematics ITWM.

Finkenstädt, B.F., Bjørnstad, O.N., Grenfell, B.T., 2002. A stochastic model for extinction and recurrence of epidemics: estimation and inference for measles outbreaks. Biostatistics 3, 493–510. doi:10.1093/biostatistics/3.4.493.

Fodor, Z., Katz, S., Kovacs, T., 2020. Why integral equations should be used instead of differential equations to describe the dynamics of epidemics. arXiv:arXiv:2004.07208.

Fraser, C., Riley, S., Anderson, R., Ferguson, N., 2004. Factors that make an infectious disease outbreak controllable. Proceedings of the National Academy of Sciences 101, 6146–6151. doi:10.1073/pnas.0307506101.

Freer, G., Pistello, M., 2008. Varicella-zoster virus infection: natural history, clinical manifestations, immunity and current and future vaccination strategies. New Microbiologica 41, 95–105.

Gao, H., Li, W., Pan, M., Han, Z., Poor, H., 2021. Modeling covid-19 with mean field evolutionary dynamics: Social distancing and seasonality. Journal of Communications and Networks 23, 314–325. doi:10.23919/JCN.2021.000032.

Gershon, A.A., Gershon, M.D., 2013. Pathogenesis and current approaches to control of varicella-zoster virus infections. Clinical Microbiology Reviews 26, 728–743. doi:10.1128/CMR.00052-13.

Greenberg, D.P., von König, C.H., Heininger, U., 2005. Health burden of pertussis in infants and children. The Pediatric Infectious Disease Journal 24, S39–43. doi:10.1097/01.inf.0000160911.65632.e1.

Greenhalgh, D., 1988. Threshold and stability results for an epidemic model with an age-structured meeting rate. Mathematical Medicine and Biology: A Journal of the IMA 5, 81–100. doi:10.1093/imammb/5.2.81.

Guerra, F., Bolotin, S., Lim, G., Heffernan, J., Deeks, S., Li, Y., Crowcroft, N., 2017. The basic reproduction number (R_0) of measles: a systematic review. The Lancet Infectious Diseases 17, e42–e428. doi:10.1016/S1473-3099(17)30307-9.

Hadeler, K., 2011. Parameter identification in epidemic models. Mathematical Biosciences 229, 185–189. doi:10.1016/j.mbs.2010.12.004.

Hethcote, H.W., Yorke, J.A., Nold, A., 1982. Gonorrhea modeling: a comparison of control methods. Mathematical Biosciences 58, 93–109. doi:10.1016/0025-5564(82)90053-0.

Heymann, D., 2008. Control of communicable diseases manual. American Public Health Association.

Hussain, Z., Das, B.C., Husain, S.A., Murthy, N.S., Kar, P., 2006. Increasing trend of acute hepatitis A in north India: need for identification of high-risk population for vaccination. Journal of Gastroenterology and Hepatology 21, 689–693. doi:10.1111/j.1440-1746.2006.04232.x.

Inthamoussou, F.A., Valenciaga, F., Núñez, G., 2022. Extended seir model for health policies assessment against the covid-19 pandemic: the case of argentina. Journal of Healthcare Informatics Research 6, 91–111. doi:10.1007/s41666-021-00110-x.

Kabanikhin, S., Krivorot'ko, O., 2020. Mathematical modeling of the wuhan coronavirus epidemic covid-2019 and inverse problems. Journal of Computational Mathematics and Mathematical Physics 60, 1950–1961. doi:https://doi.org/10.31857/S004446692011006X.

Kermack, W.O., McKendrick, A.G., 1927. A contribution to the mathematical theory of epidemics. Proceedings of the royal society of london 115, 700–721. doi:10.1007/BF02464423.

Knock, E., Whittles, L., Lees, J., Perez-Guzman, P., Verity, R., FitzJohn, R., Gaythorpe, K., Imai, N., Hinsley, W., Okell, L., Rosello, A., Kantas, N., Walters, C., Bhatia, S., Watson, O., Whittaker, C., Cattarino, L., Boonyasiri, A., Djaafara, B., Fraser, K., Fu, H., Wang, H., Xi, X., Donnelly, C., Jauneikaite, E., Laydon, D., White, P., Ghani, A., Ferguson, N., Cori, A., Baguelin, M., 2021. Key epidemiological drivers and impact of interventions in the 2020 sars-cov-2 epidemic in england. Science Translational Medicine 13, eabg4262. doi:10.1126/scitranslmed.abg4262.

Koivu-Jolma, M., Annila, A., 2018. Epidemic as a natural process. Mathematical Biosciences 299, 97–102. doi:10.1016/j.mbs.2018.03.012.

Kretzschmar, M., Wiessing, L., 2008. New challenges for mathematical and statistical modeling of hiv and hepatitis c virus in injecting drug users. AIDS 22, 1527–1537. doi:10.1097/QAD.0b013e3282ff6265.

Krivorot'ko, O., Kabanikhin, S., Zyat'kov, N., Prikhod'ko, A., Prokhoshin, N., Shishlenin, M., 2020. Mathematical modeling and forecasting of covid-19 in moscow and novosibirsk region. Numerical Analysis and Applications 13, 332–348. doi:https://doi.org/10.1134/S1995423920040047.

Marguta, R., Parisi, A., 2016. Periodicity, synchronization and persistence in pre-vaccination measles. Journal of The Royal Society Interface 13, 20160258. doi:10.1098/rsif.2016.0258.

Matsuki, A., Tanaka, G., 2019. Intervention threshold for epidemic control in susceptible-infected-recovered metapopulation models. Physical Review E 100, 022302. doi:10.1103/PhysRevE.100.022302.

Morens, D., Folkers, G., Fauci, A., 2004. The challenge of emerging and re-emerging infectious diseases. Nature 430, 242–249. doi:10.1038/nature02759.

Padmanabhan, R., Abed, H., Meskin, N., Khattab, T., Shraim, M., Al-Hitmi, M., 2021. A review of mathematical model-based scenario analysis and interventions for covid-19. Computer Methods and Programs in Biomedicine 209, 106301. doi:10.1016/j.cmpb.2021.106301.

Pesco, P., Bergero, P., Fabricius, G., Hozbor, D., 2014. Modelling the effect of changes in vaccine effectiveness and transmission contact rates on pertussis epidemiology. Epidemics 7, 13–21. doi:10.1016/j.epidem.2014.04.001.

Popkov, Y., Dubnov, Y., Popkov, A., 2021. Forecasting development of covid-19 epidemic in european union using entropy-randomized approach. IA 20, 1010–1033. doi:10.15622/20.5.1.

Puhach, O., Adea, K., Hulo, N., Sattonnet, P., Genecand, C., Iten, A., Jacquérioz, F., Kaiser, L., Vetter, P., Eckerle, I., Meyer, B., 2022. Infectious viral load in unvaccinated and vaccinated individuals infected with ancestral, delta or omicron SARS-CoV-2. Nature Medicine , 1–19doi:10.1038/s41591-022-01816-0.

Rozhnova, G., Nunes, A., 2012. Modelling the long-term dynamics of pre-vaccination pertussis. Journal of The Royal Society Interface 9, 2959–2970. doi:10.1098/rsif.2012.0432.

Russell, M.W., Gray-Owen, S.D., Jerse, A.E., 2020. Editorial: Immunity to neisseria gonorrhoeae. Frontiers in Immunology 11, 1375. doi:10.3389/fimmu.2020.01375.

Shad, A.A., Shad, W.A., 2021. Shigella sonnei: virulence and antibiotic resistance. Archives of Microbiology 203, 45–58. doi:10.1007/s00203-020-02034-3.

Shah, K., Saxena, D., Mavalankar, D., 2020. Secondary attack rate of covid-19 in household contacts: Systematic review. QJM: monthly journal of the Association of Physicians 113, 841–850. doi:10.1093/qjmed/hcaa232.

Shao, Y., Wo, J., 2020. Idm editorial statement on the 2019-ncov. Infection Disease Modelling 5, 233–234. doi:10.1016/j.idm.2020.01.003.

Silva, P., Batista, P., Lima, H., Alves, M., Guimarães, F., Silva, R., 2020. Covid-abs: An agent-based model of covid-19 epidemic to simulate health and economic effects of social distancing interventions. Chaos, Solitons & Fractals 139, 110088. doi:10.1016/j.chaos.2020.110088.

Singanayagam, A., Patel, M., Charlett, A., Bernal, J., Saliba, V., Ellis, J., Ladhani, S., Zambon, M., Gopal, R., 2020. Duration of infectiousness and correlation with RT-PCR cycle threshold values in cases of covid-19, england, january to may 2020. European Communicable Disease Bulletin 25, 2001483. doi:10.2807/1560-7917.ES.2020.25.32.2001483.

Sturniolo, S., Waites, W., Colbourn, T., Manheim, D., Panovska-Griffiths, J., 2021. Testing, tracing and isolation in compartmental models. PLOS Computational Biology 17, e1008633. doi:10.1371/journal.pcbi.1008633.

Tahan, V., Karaca, C., Yildirim, B., Bozbas, A., Ozaras, R., Demir, K., Avsar, E., Mert, A., Besisik, F., Kaymakoglu, S., Senturk, H., Cakaloglu, Y., Kalayci, C., Okten, A., Tozun, N., 2005. Sexual transmission of HCV between spouses. American Journal of Gastroenterology 100, 821–824. doi:10.1111/j.1572-0241.2005.40879.x.

Thompson, K., Kalkowska, D., 2020. Review of poliovirus modeling performed from 2000 to 2019 to support global polio eradication. Expert Review of Vaccines 19, 661–686. doi:10.1080/14760584.2020.1791093.

WHO, 2005. International health regulations, (second ed.). Technical Report. World Health Organization.

Williams, B.G., Lima, V., Gouws, E., 2011. Modelling the impact of antiretroviral therapy on the epidemic of HIV. Current HIV Research 9, 367–382. doi:10.2174/157016211798038533.

Woolthuis, R.G., Wallinga, J., van Boven, M., 2017. Variation in loss of immunity shapes influenza epidemics and the impact of vaccination. BMC Infectious Diseases 17, 632. doi:10.1186/s12879-017-2716-y.

Yang, H.M., Silveira, A.S., 1998. The loss of immunity in directly transmitted infections modeling: Effects on the epidemiological parameters. Bulletin of Mathematical Biology 60, 355–372. doi:10.1006/bulm.1997.0031.

Zatsepin, O., Bragin, A., Vlasov, V., Deryabin, A., Kaminsky, G., Karamov, E., Karmanov, A., Lebedev, S., Rykovanov, G., Samarin, S., Sokolov, A., Solomin, N., Teplykh, N., Turgyev, A., Urakov, M., Khatuntsev, K., 2021. A covid-19 agent-based model, in: Zababakhin scientific readings: a collection of materials of the XV International Conference, RFNC-VNIITF named after Academ. E. I. Zababakhin, Snezhinsk. p. 302.

Zhong, H., Wang, W., 2020. Mathematical modelling for scarlet fever with direct and indirect infections. Journal of Biological Dynamics 14, 767–787. doi:10.1080/17513758.2020.1833994.

Zhou, L., Wang, Y., Xiao, Y., Li, M., 2019. Global dynamics of a discrete age-structured sir epidemic model with applications to measles vaccination strategies. Mathematical Biosciences 308, 27–37. doi:10.1016/j.mbs.2018.12.003.

Zumla, A., Ippolito, G., McCloskey, B., Bates, M., Ansumana, R., Heymann, D., Kock, R., Ntoumi, F., 2017. Enhancing preparedness for tackling new epidemic threats. The Lancet Respiratory Medicine 5, 606–608. doi:10.1016/S2213-2600(17)30189-3.